

Supporting Information

Advancing Sustainable Lignin Valorisation: Utilizing Z-Scheme Photocatalysts for Efficient Hydrogenolysis of Lignin's β -O-4, α -O-4, and 4-O-5 Linkages under Ambient Conditions

Rajat Ghalta^a and Rajendra Srivastava^{a*}

^a*Catalysis Research Laboratory, Department of Chemistry, Indian Institute of Technology Ropar, Rupnagar, Punjab-140001, India*

*Email: rajendra@iitrpr.ac.in

*Phone: +91-1881-242175; Fax: +91-1881-223395

This Supporting information has seventy-three pages (S1-S73), and contains:

Twelve Supporting Table (Table S1-S12)

Thirty-four Supporting Figures (Figures S1-S34)

	Description	Page
	Materials	S7
	Catalyst preparation	S7
	Catalyst characterization	S10
	Catalytic reaction procedure	S11
	Apparent Quantum Yield Calculation	S13
	Photoelectrochemical measurement	S13
	Tauc plot for band gap calculations	S14
	Time-Correlated Single Photon Counting calculations	S14
	Mott-Schottky analysis calculations	S14
	Nitro blue tetrazolium (NBT) test	S15
	Terephthalic acid (THA) test	S15
Table S1	Surface elemental composition, determined from EDX analysis.	S16
Table S2	Surface area and total pore volume derived from BET analysis.	S17
Table S3	Surface elemental composition, determined from XPS analysis.	S18
Table S4	Band gap of the synthesized catalysts calculated from tauc plot.	S19
Table S5	Best fitted parameters of multiexponential components for decay curve.	S20
Table S6	AQY for photocatalytic BPE hydrogenolysis.	S21
Table S7	The photocatalytic hydrogenation for the various organic substrates.	S23
Table S8	AQY for photocatalytic PPE hydrogenolysis.	S25
Table S9	AQY for photocatalytic PPEOH hydrogenolysis.	S26
Table S10	AQY for photocatalytic DPE hydrogenolysis.	S27
Table S11	Comparative catalytic activity for photocatalytic cleavage of α -O-4 linkage in lignin modal compounds.	S28
Table S12	Comparative catalytic activity for photocatalytic cleavage of β -O-4 linkage in lignin modal compounds.	S29
Fig. S1	The digital image of photocatalytic reactor and reaction setup for the photocatalytic hydrogenolysis performed in room temperature using 150 W cool white LED (intensity = 1210 W/m ²).	S31
Fig. S2	The digital image of büchi pressure reactor and reaction setup for the	S32

	thermal hydrogenolysis of BPE.	
Fig. S3	GC-MS chromatograph for reaction mixture of BPE. (Reaction conditions -light source (150 W LED), photocatalyst 3%Pd@CN/rGO/BMO(2:1) (20 mg), reactant (0.1 mmol), IPA (5 ml)), H ₂ (2 bar) time (0.5 h)).	S33
Fig. S4	GC-MS chromatograph for reaction mixture of BPE. (Reaction conditions -light source (150 W LED), photocatalyst 3%Pd@CN/rGO/BMO(2:1) (20 mg), reactant (0.1 mmol), IPA (5 ml)), H ₂ (2 bar) time (5 h)).	S34
Fig. S5	GC-MS chromatograph for reaction mixture of PPE. (Reaction conditions -light source (150 W LED), photocatalyst 1%Pd@CN/rGO/BMO(2:1) (20 mg), reactant (0.1 mmol), IPA (5 ml)), H ₂ (2 bar) time (10 h)).	S35
Fig. S6	GC-MS chromatograph for reaction mixture of PPE. (Reaction conditions -light source (150 W LED), photocatalyst 3%Pd@CN/rGO/BMO(2:1) (20 mg), reactant (0.1 mmol), IPA (5 ml)), H ₂ (2 bar) time (20 h)).	S36
Fig. S7	GC-MS chromatograph for reaction mixture of DPE. (Reaction conditions -light source (150 W LED), photocatalyst 3%Pd@CN/rGO/BMO(2:1) (20 mg), reactant (0.1 mmol), IPA (5 ml)), H ₂ (5 bar) time (15 h)).	S37
Fig. S8	GC-MS chromatograph for reaction mixture of photocatalytic hydrogenolysis of simulated lignin bio-oil. (Reaction conditions -light source (150 W LED), photocatalyst 3%Pd@CN/rGO/BMO(2:1) (20 mg), reactant (100 mg), IPA (5 ml)), H ₂ (5 bar), time 15 h).	S38
Fig. S9	GC chromatogram of the reaction mixture of BPE hydrogenolysis demonstrating the formation of acetone in the reaction. (Reaction conditions -light source (150 W LED), photocatalyst 3%Pd@CN/rGO/BMO(2:1) (20 mg), reactant (0.1 mmol), IPA (5 ml)), H ₂ (2 bar) time 3 h).	S39
Fig. S10	FTIR spectra of CN, GO, BMO, and the composite with various combinations of CN and BMO.	S40

Fig. S11	SEM images of (a)-(b) BMO, (c)-(d) CN, (e) GO, and (f)-(g) CN/rGO/BMO.	S41
Fig. S12	Pd nanoparticles size distribution obtained from HR-TEM images of 3%Pd@CN/rGO/BMO(2:1).	S42
Fig. S13	TGA of the CN, BMO, CN/rGO/BMO, 3%Pd@CN/rGO/BMO.	S43
Fig. S14	N ₂ -adsorption/desorption isotherms of (a) BMO, CN, 0.5%Pd@CN and CN/rGO/BMO, and (b) 0.5%Pd@CN/rGO/BMO, 1%Pd@CN/rGO/BMO, 3%Pd@CN/rGO/BMO, and 5%Pd@CN/rGO/BMO.	S44
Fig. S15	XPS survey spectra of the photocatalysts (CN, BMO, and 3%Pd@CN/rGO/BMO(2:1)).	S45
Fig. S16	Tauc plots (a-e) of synthesized photocatalysts.	S46
Fig. S17	LSV spectra of photocatalyst in dark and light for (a) BMO , (b) CN, (c) CN/rGO/BMO(2:1)composites, and (d) 5%Pd@CN/rGO/BMO(2:1).	S47
Fig. S18	UPS spectra of (a) CN/rGO/BMO, (b) 0.5%Pd@CN/rGO/BMO, and, (c) 5%Pd@CN/rGO/BMO.	S48
Fig. S19	BPE hydrogenolysis (a) catalyst with different metal NPs over CN (b) 0.5 % Pd over different variation of heterojunction (d) with individual component (CN, BMO, and CN/rGO/BMO) of heterojunction 3%Pd@CN/rGO/BMO. (Reaction conditions: light source (150 W LED), catalyst amount (20 mg), BPE (0.1 mmol)), H ₂ (2 bar), time 3h, and IPA (5 ml).	S49
Fig. S20	Spectral response of 3%Pd@CN/rGO/BMO in different LEDs. (Reaction conditions: substrate (0.1 mmol), catalyst amount (20 mg), IPA (5 mL), 9W LEDs, room temperature, H ₂ (2 bar), time (6 h).	S50
Fig. S21	PPEOL hydrogenolysis was conducted with different catalyst and time interval. (Reaction conditions: light source (150 W LED), catalyst amount (20 mg), PPEOL (0.1 mmol)), H ₂ (2 bar), and IPA (5 ml).	S51
Fig. S22	(a) FTIR spectrum and, (b) XRD pattern of extracted lignin.	S52
Fig. S23	GC-MS chromatograms of lignin-MeOH solution before and after photocatalysis.	S54

Fig. S24	MS spectra of the monomers (1 to 24) obtained after the photocatalytic hydrogenolysis of real lignin.	S62
Fig. S25	(a) Comparative absorption spectra of NBT solution after light illumination for 10 min over various photocatalysts, and (b) comparative fluorescence spectra of THA solution after light illumination for 30 min over various photocatalysts.	S63
Fig. S26	(a) Transient photocurrent response, and (b) PL spectra of CN/rGO/BMO(2:1) with different variation (0%, 0.5%, 2% and 5%) in wight present of rGO precursor (GO).	S64
Fig. S27	Control experiments during BPE hydrogenolysis (a) reaction in light, dark, and different temperature using 3%Pd@CN/rGO/BMO(2:1), (b) reaction in light, dark, and different temperature using 3%Pd@SBA-15, (c) with using 1.5 mmol of electron scavenger, (d) in IPA, ACN and ACN + TEA, (e) in mixture of different ratio of IPA andACN [Reaction conditions: 3%Pd@CN/rGO/BMO(2:1) (20 mg), light source (150W LED), BPE (0.1 mmol), solvent (5 ml), time (1.5 h), and H ₂ (2 bar)].	S65
Fig. S28	Control experiments during BPE hydrogenolysis (a) reaction indifferent H ₂ concentration using 3%Pd@CN/rGO/BMO(2:1), (b) with using 1.5 mmol of OH radical scavenger (c) with using 1.5 mmol of super oxide scavenger, and (d) with using 1.5 mmol of radical scavenger [Reaction conditions: 3%Pd@CN/rGO/BMO(2:1) (20 mg), light source (150W LED), BPE (0.1 mmol), solvent (5 ml), time (1.5 h), and H ₂ (2 bar)].	S66
Fig. S29	Control experiments during PPE hydrogenolysis (a) with using 1.5 mmol of electron scavenger, and (b) in IPA, ACN, ACN + TEA, and mixture of different ratio of IPA and ACN [Reaction conditions: 3%Pd@CN/rGO/BMO(2:1) (20 mg), light source (150W LED), PPE (0.1 mmol), solvent (5 ml), time (8 h), and H ₂ (2 bar)].	S67
Fig. S30	Control experiments during DPE hydrogenolysis (a) with using 1.5 mmol of electron scavenger, and (b) in IPA, ACN, ACN + TEA, and mixture of different ratio of IPA and ACN [Reaction conditions: 3%Pd@CN/rGO/BMO(2:1) (20 mg), light source (150W LED), DPE	S68

	(0.1 mmol), solvent (5 ml), time (16 h), and H ₂ (5 bar)].	
Fig. S31	A plausible mechanism for lignin modal BPE valorisation into useful chemicals using photocatalysis as a mediator.	S69
Fig. S32	A plausible mechanism for lignin modal PPE valorisation into useful chemicals using photocatalysis as a mediator.	S70
Fig. S33	A plausible mechanism for lignin modal DPE valorisation into useful chemicals using photocatalysis as a mediator.	S71
Fig. S34	(a) Catalyst recyclability conducted at half reaction starting from ~61 %conversion [Reaction conditions: BPE (1 mmol), catalyst amount (20 mg), IPA (5 mL), 150 W LED, room temperature, time 1.5 h, H ₂ (2 bar)],	S72

Materials

$\text{Bi}(\text{NO}_3)_3 \cdot 5\text{H}_2\text{O}$, graphite powder, urea and PdCl_2 were purchased from Sigma-Aldrich. $\text{Na}_2\text{MoO}_4 \cdot 2\text{H}_2\text{O}$, KMnO_4 , H_2O_2 and HCl were purchased from Loba-chemie. All other chemicals and solvents were obtained from Merck. All the chemicals were used without any further purification.

Catalyst preparation

Synthesis of CN

A crucible was filled with 16 g of urea, a nitrogen-rich organic compound, and the crucible was covered with a lid to create a sealed environment. The crucible containing urea was then subjected to an annealing process in a muffle furnace. The temperature was increased gradually with a ramp rate of 2.5 °C per minute until reaching a temperature of 550 °C. The annealing process lasted for a duration of 3 h. After the annealing process, the resulting material was yellow. The material was transformed into a powdered form using a mortar and pestle, ensuring the complete breakdown of the solid into fine particles. The resulting powder was designated g- C_3N_4 (CN), representing graphitic carbon nitride.

Synthesis of BMO

Bi_2MO_6 (BMO) was synthesized using a solvothermal method. Firstly, 1.68 g of $\text{Bi}(\text{NO}_3)_3 \cdot 5\text{H}_2\text{O}$ was dissolved in 5 mL of ethylene glycol under continuous stirring. The solution was allowed to mix for 30 minutes to ensure complete dissolution. Then, 0.421 g of $\text{Na}_2\text{MoO}_4 \cdot 2\text{H}_2\text{O}$ was added to the solution and stirred until a transparent solution was obtained, indicating the formation of a homogeneous precursor mixture. To promote the crystallization of BMO, 20 mL of ethanol was added to the precursor solution, and the mixture was aged for 4 h, allowing for nucleation and growth of the desired phase. Subsequently, the solution was transferred into a 50 mL Teflon-lined stainless-steel autoclave to undergo a solvothermal reaction. The autoclave was sealed and heated to a temperature of 160 °C and maintained at this temperature for 20 h, promoting the formation of BMO crystals through a controlled reaction within the solvent environment. After completion of the solvothermal reaction, the autoclave was gradually cooled to room temperature. The resulting solid product was separated from the solution by centrifugation to remove any remaining liquid. The obtained solid was then subjected to multiple washing using water and ethanol to eliminate impurities and residual reactants. The washing step was crucial for the purification of the BMO material. Following the washing process, the obtained BMO material was dried in a vacuum oven at a temperature

of 50 °C for an extended period, typically overnight. This prolonged drying allowed for the complete removal of any remaining solvents, ensuring the final product was free from residual solvent.

Synthesis of GO

The 1 g of graphite powder was dispersed in a 500 ml beaker containing a mixture of acids consisting of H₂SO₄, H₃PO₄, and HNO₃, with a ratio of 70:20:10, respectively. The dispersion was achieved by stirring the mixture at a medium rotational speed to ensure a homogeneous distribution of the graphite powder. Subsequently, 6 g of KMnO₄ was added gradually to the mixture while maintaining the temperature below 5 °C using an ice bath. The solution was then subjected to a temperature of 45 °C for 2 h by immersing the beaker in an oil bath. Following this step, the beaker was returned to the ice bath, and a slow addition of 100 ml of deionized water was performed to avoid sudden temperature fluctuations. The beaker was then transferred back to the oil bath, where the temperature was maintained at 85 °C for an additional hour. Throughout the experimental procedure, the mixture was continuously stirred at a moderate rate. To conclude the experiment, a simultaneous addition of 120 ml of deionized water and 15 ml of H₂O₂ (30%) was carried out. This resulted in the reduction of permanganate and manganese dioxide, as indicated by the observable colour change from caramel brown to a greenish-yellow solution. The solution was allowed to reach room temperature and subsequently subjected to a washing step involving the addition of an extra 25 ml of a 9:1 mixture of deionized water and HCl acid. This washing process aimed to eliminate metal ions present in the solution. The mixture was then subjected to centrifugation at a speed of 5000 rpm for 30 minutes at room temperature. The washing step was repeated multiple times using deionized water to thoroughly remove any residual acid. The pH of the solution was monitored continuously, and the washing process was terminated once the solution reached a neutral pH.

Synthesis of Pd@CN

To prepare the Pd NPs supported on graphitic carbon nitride (g-C₃N₄), 600 mg of CN was combined with 100 ml of ethanol and stirred for 30 minutes to ensure uniform dispersion. Subsequently, the suspension was subjected to sonication for 3 h to promote the proper mixing and dispersion of the CN particles. During this time, the required amount of PdCl₂ was dissolved in 10 ml of ethanol, creating a PdCl₂ solution. After completing the sonication process, the PdCl₂ solution was added dropwise to the CN suspension under continuous stirring. The addition of the PdCl₂ solution facilitated the deposition of Pd species onto the CN

surface. Once the addition of the PdCl₂ solution was completed, the ethanol in the mixture was evaporated at a temperature of 80 °C, promoting the removal of the solvent. The resulting material obtained from this process exhibited a greyish appearance. This greyish material was then finely powdered using a mortar and pestle to ensure a uniform and homogeneous sample. Subsequently, the finely powdered material was transferred into a boat-type crucible. The crucible containing the material was subjected to heat treatment at 300 °C for 3 h in a gas mixture of 5% H₂ (hydrogen) and 95% Ar (argon) atmosphere. The heat treatment was performed in a tube furnace, which provided a controlled and uniform heating environment. The resulting material obtained from this process is designated as x% Pd@CN, where x% represents the percentage of Pd nanoparticles incorporated within the material. The amount of PdCl₂ taken for x% Pd is $x \times (\text{molar mass of PdCl}_2 / \text{molar mass of Pd}) \times 600$.

Synthesis of Pd@CN/rGO/BMO

In the experimental procedure, an initial mixture was prepared by combining 200 mg of BMO with 25 ml of ethanol. Subsequently, specific quantities of Pd@CN (200 mg, 300 mg, 400 mg, and 500 mg) were added to the mixture. 2 wt% of graphene oxide (GO) was introduced into the mixture. The components were thoroughly mixed through stirring for a minimum of 30 minutes. Following the stirring process, the resulting suspension underwent a sonication step for 4 h. Sonication was employed to achieve a uniform dispersion of all particles within the mixture, facilitating the breakup of aggregates and ensuring homogeneous distribution of the materials. The suspension, after sonication, was transferred to an autoclave for a solvothermal treatment at 120 °C. The solvothermal process lasted for 8 h, during which the GO was successfully reduced to reduced graphene oxide (rGO) over the heterojunction of CN and BMO. The solvothermal conditions, including the controlled temperature and duration, enabled the desired reduction process and the formation of the composite structure. Subsequent to the solvothermal treatment, the solvent remaining in the suspension was evaporated by stirring the mixture at 60 °C. The resulting material was then subjected to thorough washing with water and ethanol to eliminate any impurities or residues, ensuring the purification of the composite material. After the washing procedure, the obtained material was dried in a vacuum oven at a temperature of 50 °C for an extended period, typically overnight. This prolonged drying process facilitated the complete removal of any residual solvents, resulting in a stable and dry composite material. The resulting composite material was denoted as

$x\%Pd@CN/rGO/BMO(y:1)$, where x represents the wt % of Pd incorporated within the composite, and y signifies the composition ratio of the heterojunction.

Catalyst characterization

Powder X-ray diffraction (XRD) patterns were recorded on a Rigaku Miniflex III diffractometer (30 kV and 10 mA) with Cu K α radiation. Nitrogen-sorption measurements were performed at -200 °C by Bellsorp-MiniX, volumetric adsorption analyzer, to determine the textural properties of the catalyst. Degassing was conducted at 200 °C for 3 h in the degassing port of the adsorption apparatus. Brunauer-Emmett-Teller (BET) equation was used to calculate the surface area of the material from the adsorption data points obtained for P/P0 between 0.05-0.3, and the pore diameter was estimated using the Barret-Joyner-Halenda (BJH) model. Scanning electron microscopy (SEM) measurements were carried out on a Joel instrument at an accelerating voltage of 10 kV to explore the morphology. (TEM) was obtained for an in-depth study of material on (M/s JEOL JSM 2100) instrument operating at 200 kV. The surface composition of the catalyst was investigated by the Thermofisher scientific 'Nexsa Base' X-Ray Photoelectron Spectroscopy (XPS) instrument. The XPS, VB-XPS and UPS were conducted using the Thermofisher scientific 'Nexsa Base' X-Ray Photoelectron Spectroscopy (XPS) instrument. TGA/DSC 1 STARe SYSTEM from Mettler Toledo instrument with a temperature increment of 10 °C min⁻¹ under a nitrogen atmosphere from 27 °C to 600 °C was utilized for TGA analysis. UV-DRS study of all catalysts was performed on a UV-visible spectrophotometer of Shimadzu (UV-2600) using BaSO₄ as standard reference material. The liquid UV analysis was also conducted using a UV-visible spectrophotometer of Shimadzu (UV-2600). The fluorescence decay time was evaluated using the TCSPC instrument of DeltaFlex TCSPC Lifetime Fluorimeter.

Catalytic reaction procedure

Selective hydrogenolysis of (α -O-4 linkage) benzyl phenyl ether (BPE)

The selective hydrogenolysis of BPE was conducted in a homemade photoreactor using a 150 W LED (Fig. S1). The reactor was charged with 0.1 mmol of BPE, 20 mg catalyst, and 5 mL solvent, followed by H₂ purging thrice. Finally, the reactor was filled with 2 bar H₂, and the reaction was conducted for varied reaction intervals. The BPE conversion and product selectivity were determined using gas chromatography.

Selective hydrogenolysis of (β -O-4 linkage) 2-phenoxy-1-phenylethanol (PPE)

The selective hydrogenolysis of PPE was conducted in the presence of 150 W LED (Fig. S1). The reactor was charged with 0.1 mmol of PPE, 20 mg catalyst, and 5 mL solvent, followed by H₂ purging thrice. Finally, the reactor was filled with 2 bar H₂, and the reaction was conducted for varied reaction intervals. The BPE conversion and product selectivity were determined using gas chromatography. The hydrogenolysis of PPEOH was conducted in similar way.

Selective hydrogenolysis of (4-O-5 linkage) diphenyl ether (DPE)

The selective hydrogenolysis of BPE was conducted in a homemade photoreactor using a 150 W LED (Fig. S1). The reactor was charged with 0.1 mmol of BPE, 20 mg catalyst, and 5 mL solvent, followed by H₂ purging thrice. Finally, the reactor was filled with 5 bar H₂, and the reaction was conducted for varied reaction intervals. The DPE conversion and product selectivity were determined using gas chromatography.

Selective hydrogenolysis of lignin bio-oil

The selective hydrogenolysis of lignin bio-oil was executed in a custom-built photoreactor equipped with a 150 W LED light source (Fig. S1). The reactor was loaded with 100 μ l of simulated lignin bio-oil, 20 mg of catalyst, and 5 mL of solvent, with subsequent purging using hydrogen (H₂) three times. Subsequently, the reactor was pressurized with 5 bars of hydrogen, and the reaction was carried out for varying durations. The conversion and the selectivity of the resulting products were determined through gas chromatography.

The conversion and product selectivity were monitored by gas chromatography (GC, Yonglin 6100; BP-5; 30 m \times 0.25 mm \times 0.25 mm) using the following equations.

$$\text{Substrate conversion (\%)} = \frac{\text{Moles of substrate reacted}}{\text{Initial moles of substrate}} \times 100 \quad (\text{S1})$$

$$\text{Product selectivity (\%)} = \frac{\text{Moles of specific product formed}}{\text{Moles of substrate converted}} \times 100 \quad (\text{S2})$$

The reactant conversion and product selectivity were determined by calculating the response factor obtained from the GC calibration using a standard addition method. The standards containing a fixed concentration of n-decane with different concentrations of reactants were prepared in IPA for the reactions conducted in photochemical conditions. Solutions were injected in GC (triplicate injection), and the areas were recorded. After the analysis, the calibration curve was plotted with concentration (g/L) vs peak area, and the reactant conversion and its corresponding product selectivity were determined using the below expression.

$$\frac{Area(x)}{[x]} = F \times \frac{Area(s)}{[s]} \quad (S3)$$

Where F is the response factor, Area(x) and Area(s) are areas under the peaks for analyte and n-decane, respectively. [x] and [s] are the concentrations of analyte and n-decane, respectively.

Products were also confirmed using GC-MS (Shimadzu GCMS-QP 2010 Ultra; Rtx-5 Sil Ms; 30 m × 0.25 mm × 0.25 μm) (Fig. S3-S8). The injector and detector temperature were set at 290 °C. GC column oven temperature was programmed as follows: Initial temperature = 40 °C, hold time = 5 min followed by temperature ramping to a final temperature of 280 °C with a ramp rate of 5 °C/min. 0.2 μL of the sample was injected for the analysis.

Lignin extraction from Teak wood

Five grams of teak wood sawdust were added to a 250 mL round-bottom flask equipped with a magnetic stir bar. 40 mL IPA, 10 mL of water, and 1 mL of 37% (12 M) HCl were added to the flask. The setup was then attached to a reflux condenser, and the mixture was heated and stirred at 80 °C (oil bath temperature) for 7 h. After cooling to room temperature, the resulting solid was isolated by filtration. The filtrate was concentrated using rotary evaporation. The resulting solid was then dissolved in a minimal volume of acetone, and lignin was precipitated by adding 300 mL of water. The water was removed, and the resulting precipitate was washed with saturated aqueous Na₂SO₄ to aid flocculation. It was followed by further washing with deionized water at least five times. Finally, the product was dried overnight in a vacuum oven.

Photocatalytic hydrogenolysis of native lignin

The lignin was not completely soluble in the alcoholic solvent. The thermolytic solvolysis technique was used to render the lignin soluble in an alcoholic solvent, and according to the literature, methanol (MeOH) has the best efficiency in the thermolytic solvolysis of lignin.^{S1}

Therefore, 300 mg of extracted lignin was mixed with 10 ml of MeOH and treated at 180 °C for 2 h in 10 bar N₂ pressure using a Parr pressure reactor. After the treatment, 78% of the lignin became soluble in methanol. The insoluble residue was removed through filtration. For comparison purpose the GC MS of resulted lignin solution was taken. For comparison purposes, the GC-MS of the resulted lignin solution was taken. The lignin solution was then subjected to treatment under a 150 W LED light source in the presence of 50 mg of photocatalyst. The reaction was carried out under 5 bar H₂ pressure for 24 hours. After the reaction, the catalyst was removed from the reaction mixture through centrifugation. The obtained reaction mixture was again analysed by GC-MS and compared with the initial GC-MS spectrum to assess the reaction progress (Fig. S23).

Apparent Quantum Yield (ϕ) Calculation

The quantum yield of the reaction was calculated using eq S7, which gives the ratio between the electron involved in the reaction and the molar flow of photons introduced into the reactor. The apparent wavelength (λ) of photons was estimated from the band gap of the catalyst, determined from Tauc plots. The quantum yield calculated in this manner was not the exact value but served as a reference to compare the photo efficiency of photocatalytic system.

$$\text{Apparent Quantum Yield } (\phi) = \frac{\text{Number of reacted electron} \times 100}{\text{Number of incident photon}} \quad (\text{S4})$$

$$\text{Number of reacted electron} = \text{Reactant conversion } (\text{mol}^{-1}) \times N_A (\text{mol}) \quad (\text{S5})$$

$$\text{Number of incident photon} = \frac{\text{Light intensity } (\text{Wm}^{-2}) \times \text{Area } (\text{m}^2) \times \text{Time } (\text{s})}{\frac{h (\text{Js}) c (\text{ms}^{-1})}{\lambda (\text{m})}} \quad (\text{S6})$$

$$\phi = \frac{\text{Reactant conversion } (\text{mol}^{-1}) \times N_A (\text{mol}) \times h (\text{Js}) c (\text{ms}^{-1}) \times 100}{\text{Light intensity } (\text{Js}^{-1}\text{m}^{-2}) \times \text{Area } (\text{m}^2) \times \text{Time } (\text{s}) \times \lambda (\text{m})} \quad (\text{S7})$$

Photoelectrochemical measurement

The photoelectrochemical analyses were performed with PGSTAT302N Autolab electrochemical workstation using standard three-electrode grouping in Pyrex cell with a 0.5 M aqueous sodium sulfate solution as electrolyte. The coated photocatalyst acts as a photoanode (working electrode), Pt wire electrode as a counter electrode, and Ag/AgCl as a reference electrode. Photoanode was prepared by coating photocatalyst on glass slides containing fluorine-doped tin oxide (FTO), cleaned with acetone, rinsed with DI water, and oven-dried before use. The catalyst was coated over the FTO surface using the drop-casting method. To make a binder solution, 1.5 ml of ethanol was mixed with 1 ml of water and 40 μ l of Nafion. 20 mg of the photocatalyst was added to the binder solution and sonicated for 10 min. The binder solution was cast dropwise over the glass surface using a dropper and hotplate with a temperature of 50 °C. The electrochemical impedance measurement was conducted in the frequency range of 1 MHz to 1 Hz using a sinusoidal AC perturbation signal of 5 mV. Mott-Schottky experiment was conducted at 1000 Hz constant frequency in dark conditions. LSV and transient photocurrent measurements were carried out under dark and illumination conditions using a 300 W Xenon arc lamp (Newport-R22) with a cut-off filter ($\lambda > 420$ nm and intensity of 100 mW.cm⁻²).

Tauc plot for band gap calculations

The equation $((\alpha h\nu)^{1/r} = \beta(h\nu - E_g))$ was utilized to determine the band gap. The value of r is contingent on the transition nature, where $r = 1/2$ is appropriate for direct and $r = 2$ signifies indirect transitions. The $(\alpha h\nu)^{1/r}$ vs. $(h\nu)$ plots with $r = 1/2$, enabling estimation of the band-gap for direct allowed transitions by straight line extrapolation in the case of CN and BMO.

Time-Correlated Single Photon Counting calculations

The data analysis employed double-exponential fitting to determine the average lifetimes and

their percentage contributions, employing the equation $y = y_0 + \sum_{i=1}^n \alpha_i e^{-\left(\frac{t}{\tau_i}\right)}$. To calculate

$$\langle \tau \rangle = \frac{\sum_{i=1}^n \alpha_i \tau_i^2}{\sum_{i=1}^n \alpha_i \tau_i}$$

the average decay time, $\langle \tau \rangle$, the

) was utilised, and $\sum \alpha_i$ was normalised to 1.

Mott-Schottky analysis calculations

This method involved the relation $1/C^2 = 2 [V - V_{fb} - (k_b T/e)] / (\epsilon \epsilon_0 e A^2 N_d)$. Plots of $1/C^2$ vs. applied potential were constructed. All the materials possess a positive slope, indicating their n-type semiconducting behaviour. The MS plots' x-intercepts yielded the flat-band position (E_{fb}) (Fig. 5f). In n-type semiconductors, the E_{fb} lies below to conduction band (CB) edge. The E_{fb} values were used to determine the position of the CB edge (E_{CB}) through the relation $E_{CB} = E_{fb} - 0.1$ V. Potential values were standardized using the equation ($E_{NHE} = E_{Ag/AgCl} + 0.196$), and Table S3 presents the calculated E_{CB} vs. NHE values for all the material. Finally, the valence band positions (E_{VB}) were obtained by applying the relation $E_{VB} = E_{CB} + E_g$, where E_{CB} represents the conduction band potential and E_g is the band gap.

Nitro blue tetrazolium (NBT) test

10 mL of 2.5×10^{-5} M aqueous solution of NBT was mixed with the 5 mg of the catalyst. The mixture was illuminated with light under continuous stirring. After 10 min, the catalyst was separated from the solution using a centrifuge. The solution was monitored using a UV-visible spectrophotometer, and its absorbance for NBT was compared with the neat stock solution. A decreased absorbance peak of NBT after light illumination confirms the capability of the photocatalyst for generating $\cdot O_2^-$.

Terephthalic acid (THA) test

The 5×10^{-3} M aqueous solution of THA was prepared with a small amount of NaOH to make THA soluble in an aqueous medium. 20 mg of catalyst was mixed with the 20 ml of THA solution and exposed to light for 30 min. Then catalyst was separated from the solution using a centrifuge. The clear solution was monitored using a fluorescence spectrophotometer with an excitation wavelength of 330 nm. The emission peak at 425 nm confirms 2-hydroxyl terephthalic acid in the reaction mixture. The OH radicals react with THA (non-fluorescent) and convert it into 2-hydroxyl terephthalic acid (fluorescent). The emission peak of the reaction mixture was compared with the stock solution.

Table S1. Surface elemental composition, determined from EDX analysis.

S.N.	Catalyst	Wt %					
		Pd	Bi	Mo	C	N	O
1	0.5%Pd@CN/rGO/BMO(2:1)	0.4	32.2	6.3	16.3	38.8	6.0
2	1%Pd@CN/rGO/BMO(2:1)	1.2	31.8	6.0	16.1	38.4	6.5
3	3%Pd@CN/rGO/BMO(2:1)	2.3	31.7	5.9	15.8	38.5	5.8
4	5%Pd@CN/rGO/BMO(2:1)	4.8	31.1	5.5	15.3	38.2	5.1

Table S2. Textural properties of the photocatalysts of this study.

S.N.	Catalyst	S_{BET} (m²g⁻¹)	Total pore vol. (cm³g⁻¹)
1	BMO	24	0.50
2	CN	43	0.28
3	0.5%Pd@CN	61	0.26
4	CN/rGO/BMO(2:1)	38	0.24
5	0.5%Pd@CN/rGO/BMO(2:1)	51	0.23
6	1%Pd@CN/rGO/BMO(2:1)	53	0.21
7	3%Pd@CN/rGO/BMO(2:1)	59	0.19
8	5%Pd@CN/rGO/BMO(2:1)	60	0.17

S_{BET} = BET Surface area, TPV= Total pore volume.

Table S3. Surface elemental composition, determined from XPS analysis.

S.N.	Catalyst	Surface Atomic (%)					
		Pd (283.9 eV)	Bi (160 eV)	Mo (240 eV)	C (286.9 eV)	N (398.3 eV)	O (531.0 eV)
1	0.5%Pd@CN/rGO/BMO(1:2)	0.14	1.3	1.02	41.32	47.43	8.79
2	1%Pd@CN/rGO/BMO(1:2)	0.30	1.23	0.96	41.56	46.32	9.63
3	3%Pd@CN/rGO/BMO(1:2)	0.83	1.17	0.66	41.43	45.87	10.04
4	5%Pd@CN/rGO/BMO(1:2)	1.47	1.38	0.98	41.19	45.05	9.93

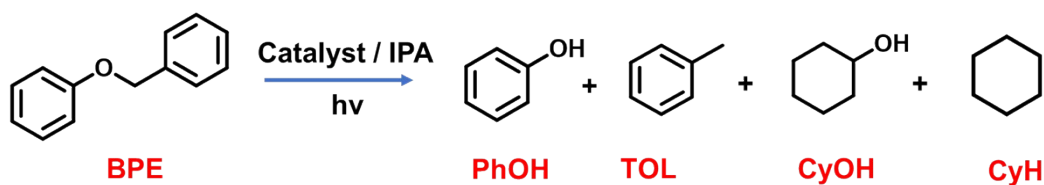
Table S4. Band gap of the synthesized catalysts calculated from tauc plot.

Entry	Catalyst	Band gap
1	BMO	2.64
2	CN	2.76
4	CN/rGO/BMO(2:1)	2.72
5	0.5%Pd@CN/rGO/BMO(2:1)	2.79
6	1%Pd@CN/rGO/BMO(2:1)	2.80
7	3%Pd@CN/rGO/BMO(2:1)	2.83
8	5%Pd@CN/rGO/BMO(2:1)	2.84

Table S5 Best fitted parameters of multiexponential components for decay curve.

Entry	Catalyst	Pre-exponential functions			Decay lifetimes (ns)				Fractional contribution (%)		
		α_1	α_2	α_3	τ_1	τ_2	τ_3	$\langle\tau\rangle$	f_1	f_2	f_3
1	CN	40	17	43	1.9812	4.3654	0.2025	2.98	48.9	45.8	5.3
2	BMO	37	16	47	2.0253	5.4842	0.9552	3.26	36.1	42.3	21.6
3	CN/rGO/BMO(2:1)	43	15	42	2.1253	6.1235	0.5263	3.74	44.5	44.7	10.8
4	3%Pd@CN/rGO/BMO(2:1)	45	20	35	2.1285	6.2934	0.5619	4.17	39.7	52.2	8.1

Table S6 AQY for photocatalytic BPE hydrogenolysis.

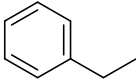
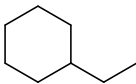
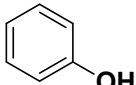
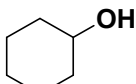
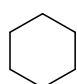
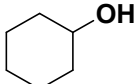
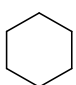
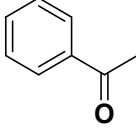
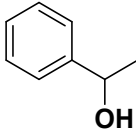
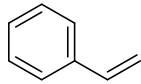
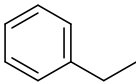
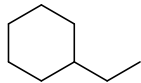
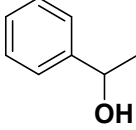
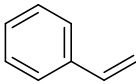
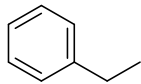
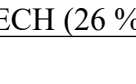


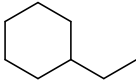
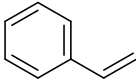
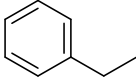
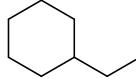
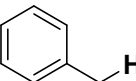
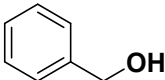
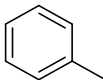
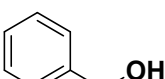
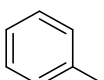
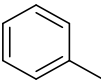
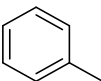
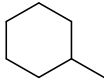
Entry	Catalyst	Time	Conv. (%)	Product Selectivity (%)				AQY
				TOL	PhOH	CyOH	CyH	
1	CN	3h	1.0	52.3	47.7	-	-	2×10^{-3}
2	BMO	3h	3.0	52.1	47.9	-	-	7×10^{-3}
3	0.5%Pd@CN	3h	38.6	51.5	48.5	-	-	86×10^{-3}
4	0.5%Ru@CN	3h	24.3	52.3	47.7	-	-	54×10^{-3}
5	0.5%Ni@CN	3h	3.8	53.1	46.9	-	-	8×10^{-3}
6	0.5%Co@CN	3h	2.3	52.8	47.2	-	-	5×10^{-3}
7	0.5%Pd@CN/rGO/BMO(1:1)	3h	64.6	51.8	48.2	-	-	142×10^{-3}
8	0.5%Pd@CN/rGO/BMO(1.5:1)	3h	72.6	53.0	47.0	-	-	159×10^{-3}
9	0.5%Pd@CN/rGO/BMO(2:1)	3h	78.3	50.8	49.2	-	-	172×10^{-3}

10	0.5%Pd@CN/rGO/BMO(2.5:1)	3h	67.1	51.1	48.9	-	-	147×10^{-3}
11	CN/rGO/BMO(2:1)	3h	6.0	51.3	48.7	-	-	12×10^{-3}
12	1%Pd@CN/rGO/BMO(2:1)	3h	92.3	51.7	48.3			209×10^{-3}
13	3%Pd@CN/rGO/BMO(2:1)	3h	~100	51.2	44.1	4.7		219×10^{-3}
14	3%Pd@CN/rGO/BMO(2:1)	6h	~100	50.7	15.0	12.0	22.3	110×10^{-3}
15	3%Pd@CN/rGO/BMO(2:1)	16h	~100	51.5	-	-	48.5	41×10^{-3}

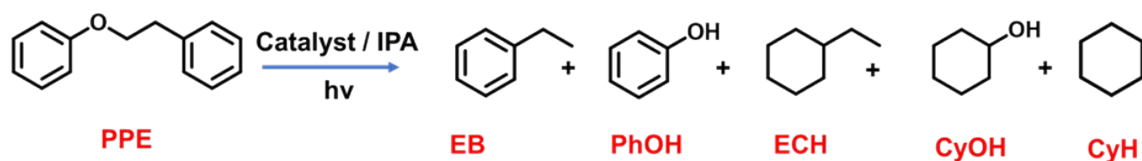
Reaction conditions: light source (150 W LED), photocatalyst (20 mg), reactant (0.1 mmol), IPA (5 ml), H₂ (2 bar). AQY was calculated using Equation S4-S7 (SI).

Table S7 The photocatalytic hydrogenation for the various organic substrates.

Substrate	Catalyst	Time	Conv. (%)	Product Selectivity	Product Selectivity	AQY
 EB	3%Pd@CN/rGO/BMO(2:1)	12h	95 %	ECH (100 %) 		52×10^{-3}
 PhOH	3%Pd@CN/rGO/BMO(2:1)	6h	~100 %	CyOH (57 %) 	CyH (43 %) 	111×10^{-3}
 CyOH	3%Pd@CN/rGO/BMO(2:1)	10h	~100 %	CyH (100 %) 	-	65×10^{-3}
 AcPh	3%Pd@CN/rGO/BMO(2:1)	6h	~97 %	PEA (15 %) 	STY (3 %) 	106×10^{-3}
				EB (75 %) 	ECH (7 %) 	
 PEA	3%Pd@CN/rGO/BMO(2:1)	6h	~100 %	STY (5 %) 	EB (69 %) 	110×10^{-3}
				ECH (26 %) 		

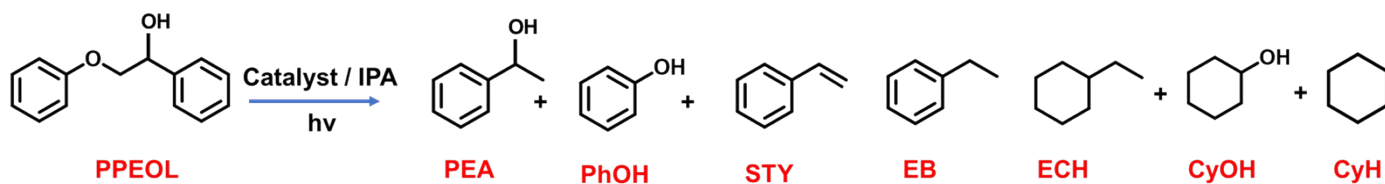
						
 STY	3%Pd@CN/rGO/BMO(2:1)	6h	~ 100 %	EB (65 %) 	ECH (35 %) 	110×10^{-3}
 BZAL	3%Pd@CN/rGO/BMO(2:1)	4 h	~100 %	BnOH (42 %) 	TOL (58) 	164×10^{-3}
 BnOH	3%Pd@CN/rGO/BMO(2:1)	4 h	~100 %	TOL (100%) 		164×10^{-3}
 TOL	3%Pd@CN/rGO/BMO(2:1)	4 h	~1 %			-
 TOL	3%Pd@CN/rGO/BMO(2:1)	16 h	9 %	MCY (100%) 		4×10^{-3}

Reaction conditions: Light source (150 W LED), photocatalyst (20 mg), reactant (0.1 mmol), IPA (5 ml)), H₂ (2 bar) AQY was calculated using Equation S4-S7 (SI).

Table S8 AQY for photocatalytic PPE hydrogenolysis.

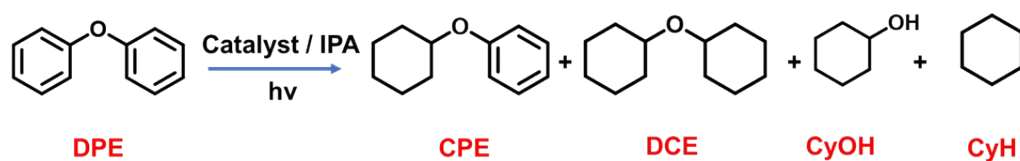
Entry	Catalyst	Time	Conv. (%)	Product Selectivity (%)					AQY
				EB	PhOH	ECH	CyOH	CyH	
1	0.5%Pd@CN/rGO/BMO(2:1)	16 h	80.2	51.8	48.2	-	-	-	32×10^{-3}
2	0.5%Pd@CN/rGO/BMO(2:1)	24 h	100	52.5	47.5	-	-	-	27×10^{-3}
3	1%Pd@CN/rGO/BMO(2:1)	16 h	95.8	50	48.4	0.5	1.1	-	39×10^{-3}
4	1%Pd@CN/rGO/BMO(2:1)	24 h	100	48.2	46.2	2.1	3.5	-	27×10^{-3}
5	3%Pd@CN/rGO/BMO(2:1)	16 h	100	32.4	22.0	18.5	20.8	6.3	41×10^{-3}
6	3%Pd@CN/rGO/BMO(2:1)	24 h	100	25.6	11.6	25.7	19.5	17.6	27×10^{-3}
7	5%Pd@CN/rGO/BMO(2:1)	16 h	100	11.7	7.6	40.3	12.9	27.5	41×10^{-3}
8	5%Pd@CN/rGO/BMO(2:1)	24 h	100	-	-	50.9	6.5	42.6	27×10^{-3}

Reaction conditions: Light source (150 W LED), photocatalyst (20 mg), reactant (0.1 mmol), IPA (5 ml), H₂ (2 bar). AQY was calculated using Equation S4-S7 (SI).

Table S9 AQY for photocatalytic PPEOH hydrogenolysis.

Entry	Catalyst	Time	Conv. (%)	Product Selectivity (%)							AQY
				PEA	PhOH	STY	EB	ECH	CyOH	CyH	
1	0.5%Pd@CN/rGO/BMO(2:1)	12 h	69.8	25.2	48.2	4.5	22.1	-	-	-	38×10^{-3}
2	0.5%Pd@CN/rGO/BMO(2:1)	16 h	78.9	16.5	49.9	2.5	31.1	-	-	-	32×10^{-3}
3	1%Pd@CN/rGO/BMO(2:1)	12 h	88.7	14.6	49.5	3.2	32.7	-	-	-	48×10^{-3}
4	1%Pd@CN/rGO/BMO(2:1)	16 h	98.5	5.6	42.3	1.3	44.6		6.3		40×10^{-3}
5	3%Pd@CN/rGO/BMO(2:1)	12 h	100	3.2	26.2	0.9	35.3	11.6	21.6	1.2	55×10^{-3}
6	3%Pd@CN/rGO/BMO(2:1)	16 h	100	0.8	12.5	0	31.9	18.5	26.5	9.8	41×10^{-3}
7	5%Pd@CN/rGO/BMO(2:1)	12 h	100	-	8.5	-	24.2	26.5	18.2	22.6	55×10^{-3}
8	5%Pd@CN/rGO/BMO(2:1)	16 h	100	-	-	-	11.2	39.6	14.6	34.6	41×10^{-3}

Reaction conditions: light source (150 W LED), photocatalyst (20 mg), reactant (0.1 mmol), IPA (5 ml), H₂ (2 bar). AQY was calculated using Equation S4-S7 (SI).

Table S10 AQY for photocatalytic DPE hydrogenolysis.

Entry	Catalyst	Time	Conv. (%)	Product Selectivity (%)				AQY
				CPE	DCE	CyOH	CyH	
1	0.5%Pd@CN/rGO/BMO(2:1)	16 h	4.6	5.6	15.2	37.4	41.8	2×10^{-3}
2	0.5%Pd@CN/rGO/BMO(2:1)	24 h	7.0	4.8	14.3	36.1	44.8	2×10^{-3}
3	1%Pd@CN/rGO/BMO(2:1)	16 h	17.5	4.2	13.1	35.5	47.2	7×10^{-3}
4	1%Pd@CN/rGO/BMO(2:1)	24 h	22.3	3.6	11.5	33.2	51.7	6×10^{-3}
5	3%Pd@CN/rGO/BMO(2:1)	16 h	36.7	3.1	10.2	30.1	56.6	15×10^{-3}
6	3%Pd@CN/rGO/BMO(2:1)	24 h	49.3	1.9	7.2	21.6	69.3	13×10^{-3}
7	5%Pd@CN/rGO/BMO(2:1)	16 h	57.2	1.8	6.1	2.0	72.1	23×10^{-3}
8	5%Pd@CN/rGO/BMO(2:1)	24 h	74.6		2.0	4.6	93.4	20×10^{-3}

Reaction conditions: light source (150 W LED), photocatalyst (20 mg), reactant (0.1 mmol), IPA (5 ml), H₂ (5 bar). AQY was calculated using Equation S4-S7 (SI).

Table S11 Comparative catalytic activity for photocatalytic cleavage of α -O-4 linkage in lignin modal compounds.

S. N.	Catalyst	Reaction Condition	Conversion (%)	Selectivity(S)/Yield(Y) (%)			AQY	Ref.
				Aromatic		Aliphatic		
				TOL	PhOH	CyH		
1	2.5Au-ASN-Ni ²⁺	Photocatalyst (20 mg), BPE (0.05 mmol), KOH (0.15 mmol), and 2 mL (IPA) as solvent, argon atmosphere. halogen lamp and the reaction was conducted at 90°C	98	~50(S)	~50(S)	-	-	S2
2	TiN NPs	20 mg of TiN NPs as the photocatalyst, 0.05 mmol of reactant, 0.15 mmol of KOH, 2 mL of isopropanol as the solvent, reaction temperature of 100 °C, visible light intensity of 0.5 W/cm ² , reaction time of 14 h, and 1 atm of argon atmosphere.	11	~50(S)	~50(S)	-	-	S3
4	1%Pd@CN/rGO/BMO (2:1)	Photocatalyst (20 mg), BPE (0.1 m mol mg), IPA (5 mL), H ₂ (2 bar), and 150 W LEDs, time 3h.	92.3	51.7(S)	48.3(S)	-	0.20	This Study
5	3%Pd@CN/rGO/BMO (2:1)	Photocatalyst (20 mg), PPEOL (0.1 m mol mg), IPA (5 mL), H ₂ (2 bar), and 150 W LEDs, time 16h.	100		51.5(S)	48.5(S)	0.04	This Study

Table S12 Comparative catalytic activity for photocatalytic cleavage of β -O-4 linkage in lignin modal compounds.

S. N.	Catalyst	Reaction Condition	Conversion (%)	Selectivity(S)/Yield(Y) (%)					AQY	Ref.
				Aromatic			Aliphatic			
				PhOH	EB	AP	ECH	CyH		
1	Zn ₄ In ₂ S ₇	Photocatalyst (10 mg), PPEOL (0.10 mmol), CH ₃ CN/H ₂ O (5.0 mL, 1:1 v/v), N ₂ atmosphere, 4 h, Xe lamp (λ =400–780 nm),	100	82 (Y)	-	86(Y)	-	-	0.0004	S4
2	ZnIn ₂ S ₄	Photocatalyst (5 mg), PPEOL (0.10 mmol), 1.0 mL of CH ₃ CN, 9.6 W blue LEDs (455 nm), 42 °C, 4 h.	>99	90(Y)	-	83(Y)	-	-	-	S5
3	ZnIn ₂ S ₄	Photocatalyst (10 mg), PPEOL (10 mg), (CH ₃ CN:H ₂ O = 2:3), visible light irradiation (0.35 W/cm ²), Room temperature (20–25 °C), 90 min.	100	93.7(Y)	-	91.9(Y)	-	-	-	S6
4	TiN NPs	Photocatalyst (20 mg), PPEOL (0.05 mmol), 0.15 mmol of KOH, 2 mL of isopropanol as the solvent, reaction temperature of 100 °C, visible light intensity of 0.5 W/cm ² , reaction time of 14 h, and 1 atm of argon atmosphere.	82.0	49(S)	50 (styrene)(S)	-	-	-	0.015	S3
5	CdS	0.01 g of photocatalyst, 3 mL of solvent(CTAB-15), 100 W blue lamps (455 nm), N ₂ atmosphere, 30 min, 15–40 °C	99.8	81.79(Y)	-	74.65(Y)	-	-	-	S7
6	Ni/CdS	Photocatalyst (20 mg), PPEOL (5 mmol), in 10 mL of CH ₃ CN/0.1 N KOH at room temperature, time 3h irradiated under royal blue light (λ = 440–460 nm).	100	~100(Y)	-	~100(Y)	-	-	-	S8
8	CdS-C ₃ N ₄	Photocatalyst (5 mg), PPEOL (10 mg), and 2 mL of solvent (1.6 mL of acetonitrile and 0.4 mL of H ₂ O) were added into a quartz tube (20 mL), respectively, purged with Ar. After illumination with 50 W, 455 nm for 1.5 h.	~100	~85(Y)	-	~75(Y)	-	-	-	S9
9	Ag ₂ S(2%)@CdS	Photocatalyst (1 mg), PPEOL (10 mg), CH ₃ CN (1.0 mL), Ar (1 atm), and 6 W blue LEDs.	100	~88(Y)	-	~76(Y)	-	-	-	S10
10	Cd _x Zn _{1-x} S	0.1 mmol of model compound, 0.01 g of photocatalyst ZCS-70, 5 mL of CH ₃ CN except entry 6, 300 W Xe-lamp, 17–23 °C, illumination for 2 h.	63.21	49.74 (Y)	-	23.71(Y)	-	-	-	S11

12	CdS@Cd _x Zn _{1-x} S@ZnS Gradient Alloyed QDs	0.01 mmol/L of PP-ol, 10 mg of CdS@Cd _x Zn _{1-x} S@ZnS QDs photocatalyst, 0.1 mmol/L of acid, 10 mL of solvent MeCN, blue LED irradiation (10 W), room temperature, N ₂ atmosphere.	~ 90	70(Y)		65(Y)					S12
13	1%Pd@CN/rGO/BMO(2:1)	Photocatalyst (20 mg), PPE (0.1 m mol mg), IPA (5 mL), H ₂ (2 bar), and 150 W LEDs, time 16h.	95.8	49.5(S)	50.5(S)	-	-	-	0.04		This Study
14	5%Pd@CN/rGO/BMO(2:1)	Photocatalyst (20 mg), PPE (0.1 m mol mg), IPA (5 mL), H ₂ (2 bar), and 150 W LEDs, time 24h.	100	-	-	-	50.9(S)	42.6(S)	0.03		This Study
15	1%Pd@CN/rGO/BMO(2:1)	Photocatalyst (20 mg), PPEOL (0.1 m mol mg), IPA (5 mL), H ₂ (2 bar), and 150 W LEDs, time 16h.	98.5	42.3(S)	44.6(S)	-	-	-	0.04		This Study
16	5%Pd@CN/rGO/BMO(2:1)	Photocatalyst (20 mg), PPEOL (0.1 m mol mg), IPA (5 mL), H ₂ (2 bar), and 150 W LEDs, time 16h.	100		11.2(S)		39.6(S)	34.6(S)	0.04		This Study

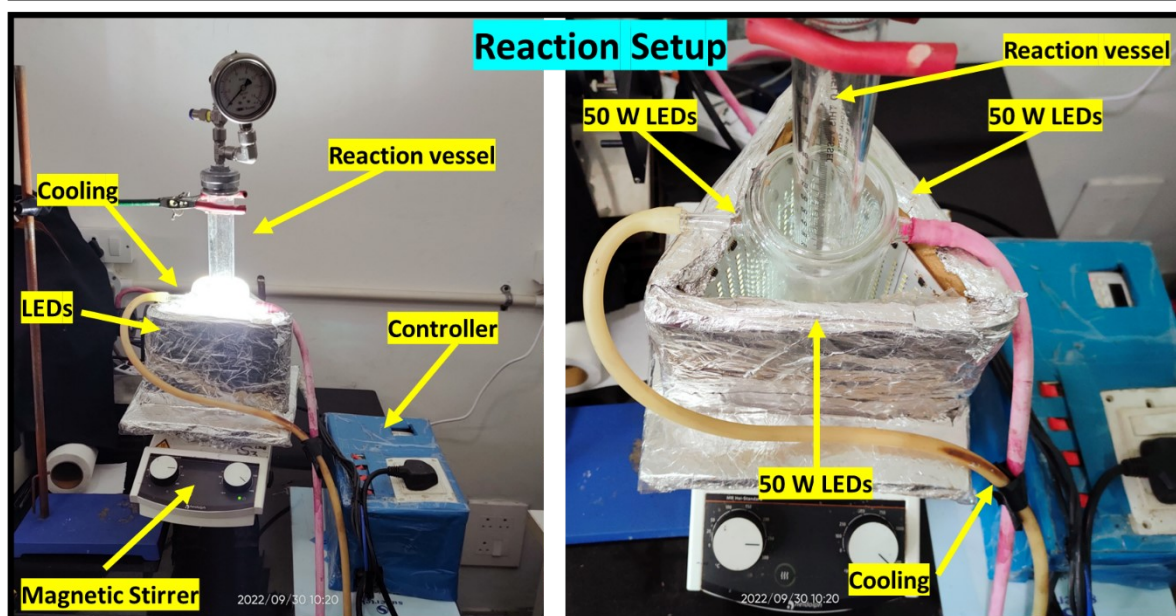
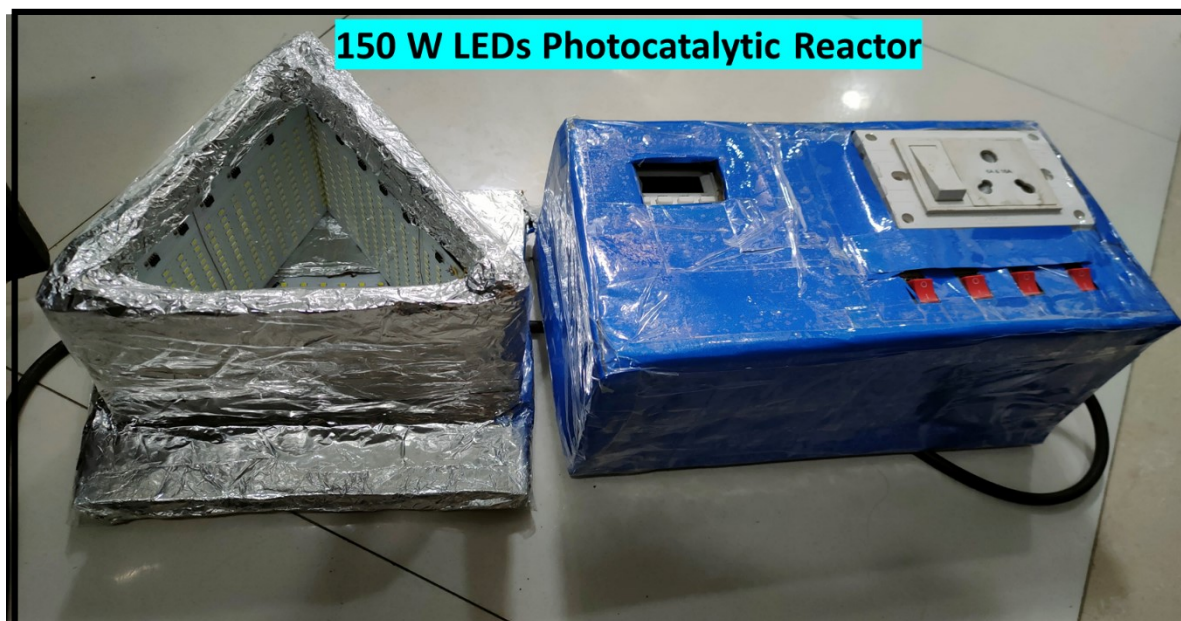


Fig. S1. The digital image of photocatalytic reactor and reaction setup for the photocatalytic hydrogenolysis performed in room temperature using 150 W cool white LED (intensity = 1210 W/m²).



Fig. S2. The digital image of Büchi pressure reactor and reaction setup for the thermal hydrogenolysis of BPE.

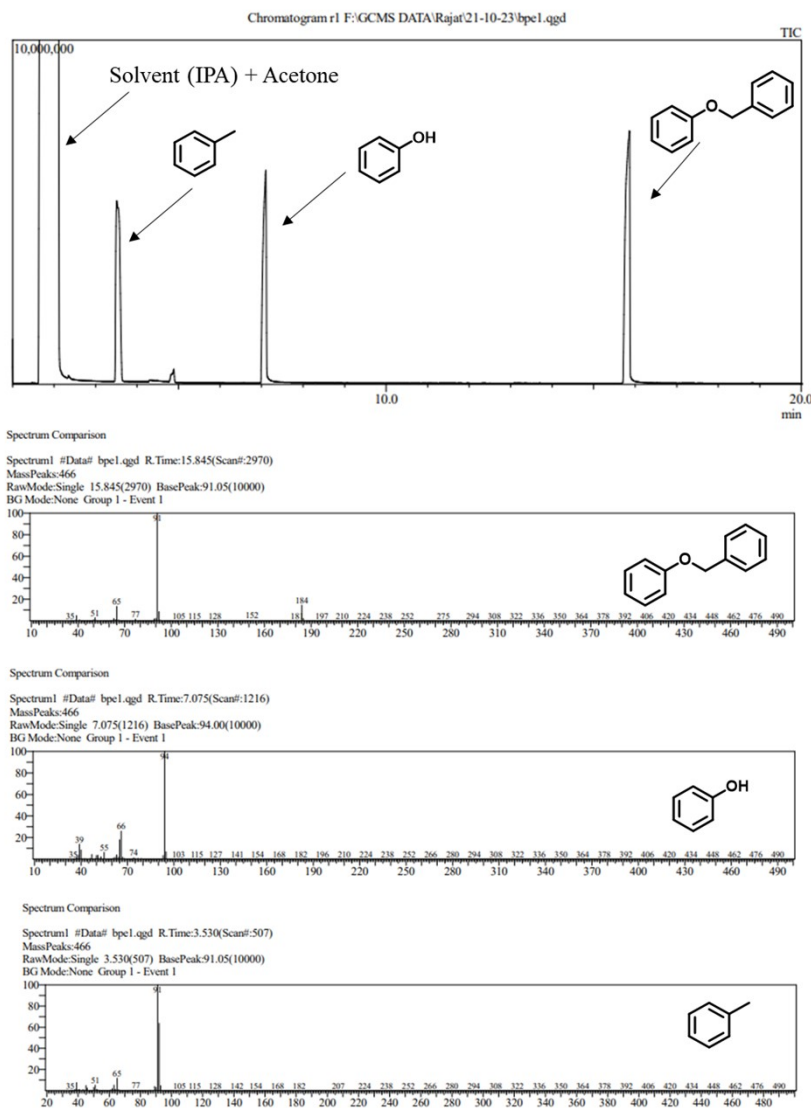


Fig. S3. GC-MS chromatograph for reaction mixture of BPE. (Reaction conditions -light source (150 W LED), photocatalyst 3%Pd@CN/rGO/BMO(2:1) (20 mg), reactant (0.1 mmol), IPA (5 ml)), H₂ (2 bar) time (0.5 h)).

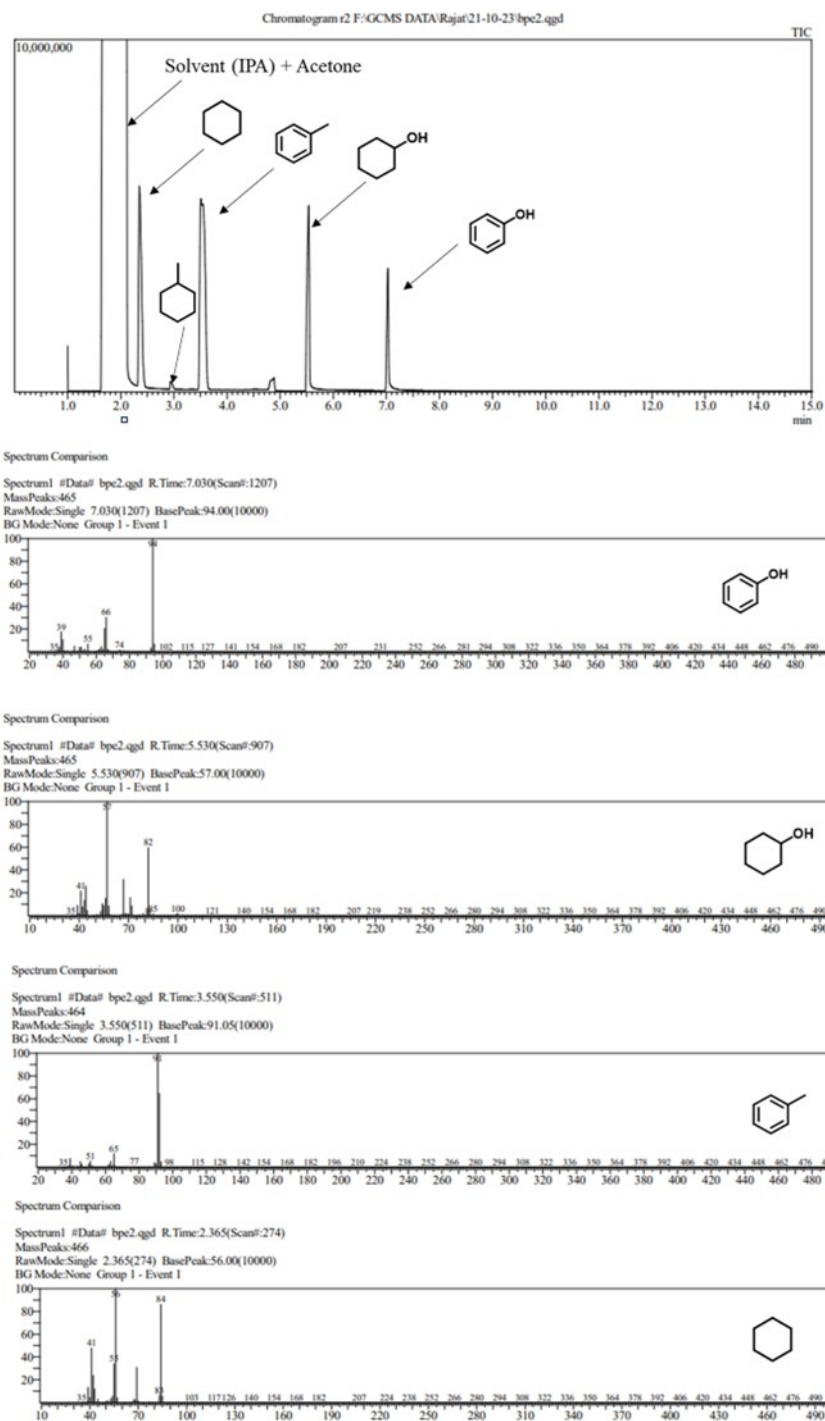
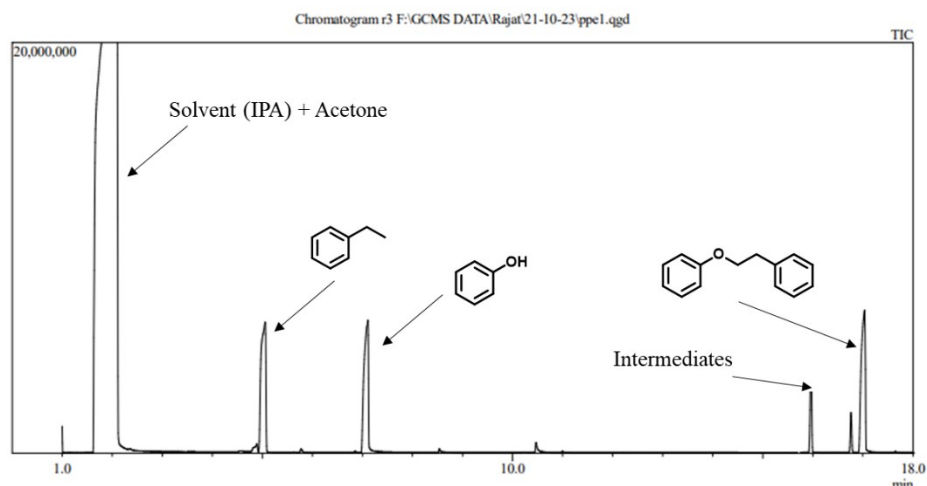
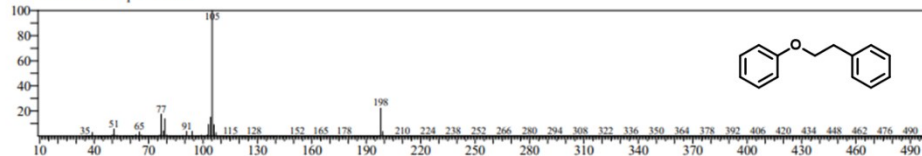


Fig. S4. GC-MS chromatograph for reaction mixture of BPE. (Reaction conditions -light source (150 W LED), photocatalyst 3%Pd@CN/rGO/BMO(2:1) (20 mg), reactant (0.1 mmol), IPA (5 ml), H₂ (2 bar) time (5 h)).



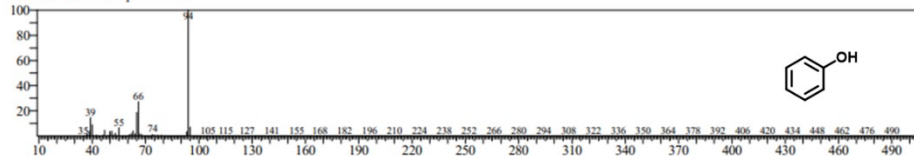
Spectrum Comparison

Spectrum1 #Data# ppe1.qgd R.Time:17.010(Scan#:3203)
 MassPeaks:466
 RawMode:Single 17.010(3203) BasePeak:105.05(10000)
 BG Mode:None Group 1 - Event 1



Spectrum Comparison

Spectrum1 #Data# ppe1.qgd R.Time:7.055(Scan#:1212)
 MassPeaks:466
 RawMode:Single 7.055(1212) BasePeak:94.00(10000)
 BG Mode:None Group 1 - Event 1



Spectrum Comparison

Spectrum1 #Data# ppe1.qgd R.Time:5.015(Scan#:804)
 MassPeaks:466
 RawMode:Single 5.015(804) BasePeak:91.00(10000)
 BG Mode:None Group 1 - Event 1

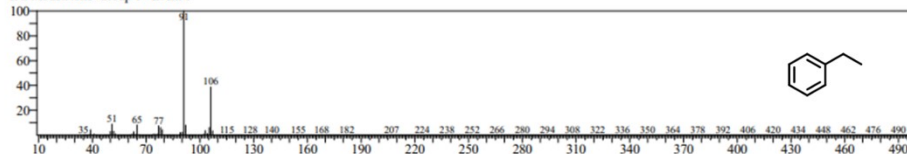
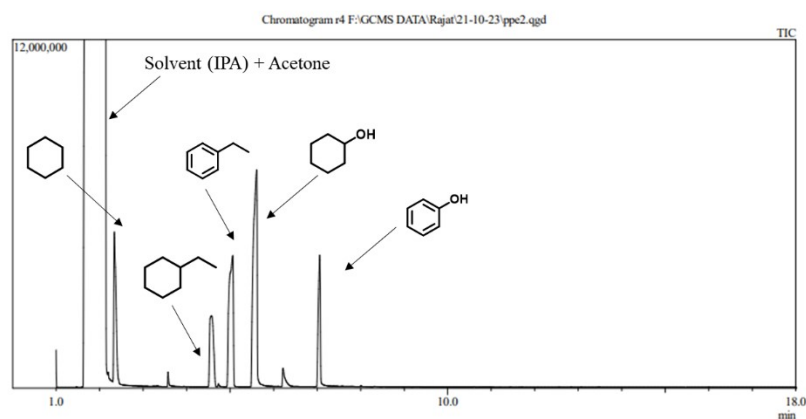
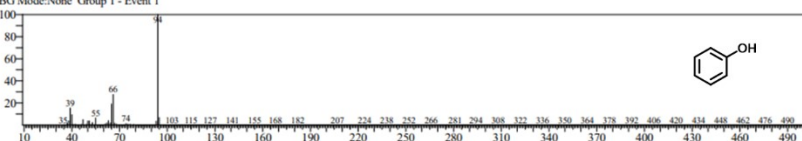


Fig. S5. GC-MS chromatograph for reaction mixture of PPE. (Reaction conditions -light source (150 W LED), photocatalyst 1%Pd@CN/rGO/BMO(2:1) (20 mg), reactant (0.1 mmol), IPA (5 ml), H₂ (2 bar) time (10 h)).



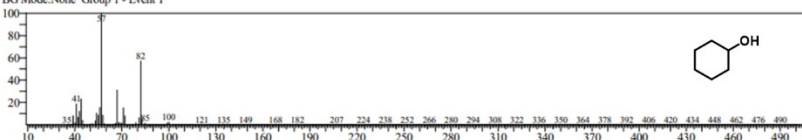
Spectrum Comparison

Spectrum1 #Data# ppe2.qgd R.Time:7.055(Scan#:1212)
 MassPeaks:466
 RawMode:Single 7.055(1212) BasePeak:94.00(10000)
 BG Mode:None Group 1 - Event 1



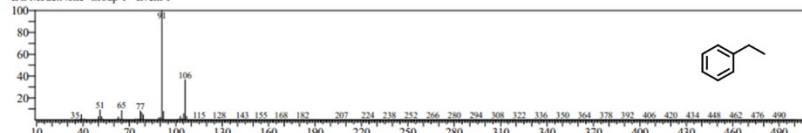
Spectrum Comparison

Spectrum1 #Data# ppe2.qgd R.Time:5.575(Scan#:916)
 MassPeaks:466
 RawMode:Single 5.575(916) BasePeak:57.00(10000)
 BG Mode:None Group 1 - Event 1



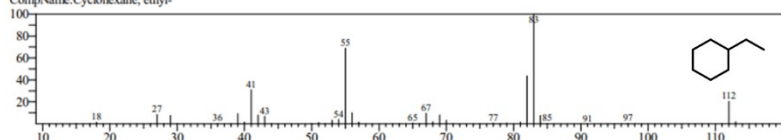
Spectrum Comparison

Spectrum1 #Data# ppe2.qgd R.Time:5.030(Scan#:807)
 MassPeaks:466
 RawMode:Single 5.030(807) BasePeak:91.00(10000)
 BG Mode:None Group 1 - Event 1



Compound Information

Entry:7561 Library:NIST17.LIB
 Formula:C8H16 CAS:1678-91-7 MolWeight:112 RetIndex:880
 CompName:Cyclohexane, ethyl-



Spectrum Comparison

Spectrum1 #Data# ppe2.qgd R.Time:2.355(Scan#:272)
 MassPeaks:466
 RawMode:Single 2.355(272) BasePeak:56.00(10000)
 BG Mode:None Group 1 - Event 1

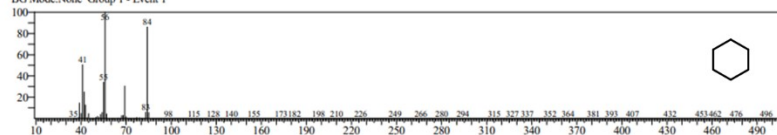


Fig. S6. GC-MS chromatograph for reaction mixture of PPE. (Reaction conditions -light source (150 W LED), photocatalyst 3%Pd@CN/rGO/BMO(2:1) (20 mg), reactant (0.1 mmol), IPA (5 ml), H₂ (2 bar) time (20 h)).

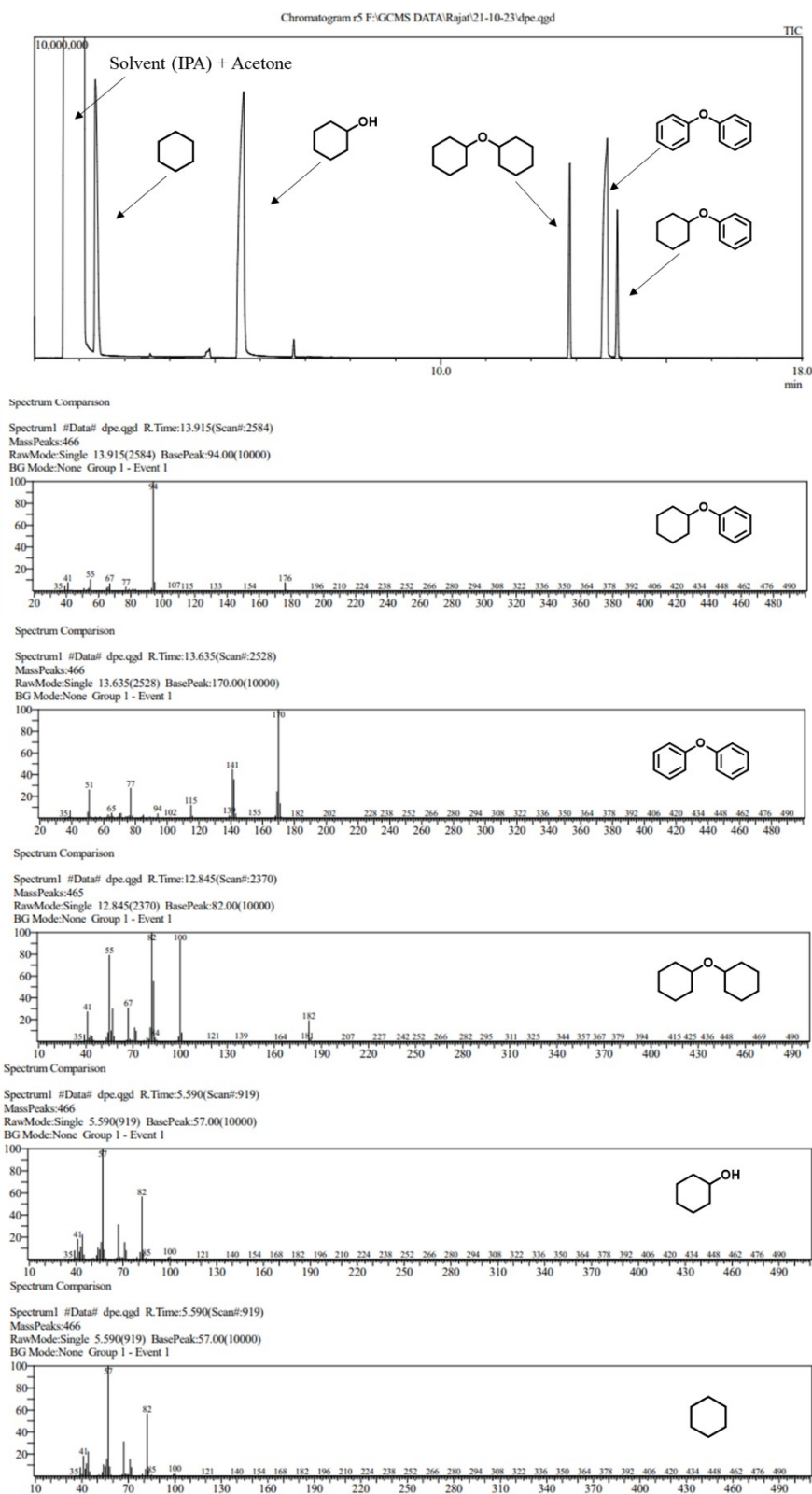


Fig. S7. GC-MS chromatograph for reaction mixture of DPE. (Reaction conditions -light source (150 W LED), photocatalyst 3%Pd@CN/rGO/BMO(2:1) (20 mg), reactant (0.1 mmol), IPA (5 ml)), H₂ (5 bar) time (15 h).

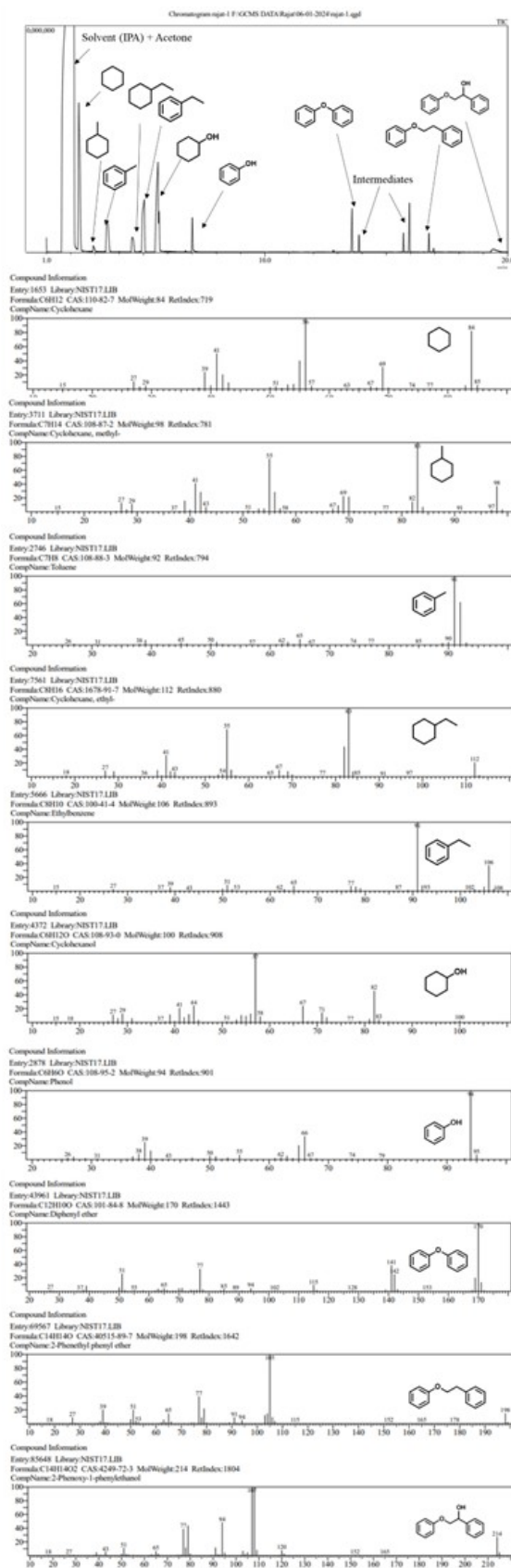


Fig. S8. GC-MS chromatogram for reaction mixture of photocatalytic hydrogenolysis of simulated lignin bio-oil. (Reaction conditions -light source (150 W LED), photocatalyst

3%Pd@CN/rGO/BMO(2:1) (20 mg), reactant (100 mg), IPA (5 ml)), H₂ (5 bar), time (15 h).

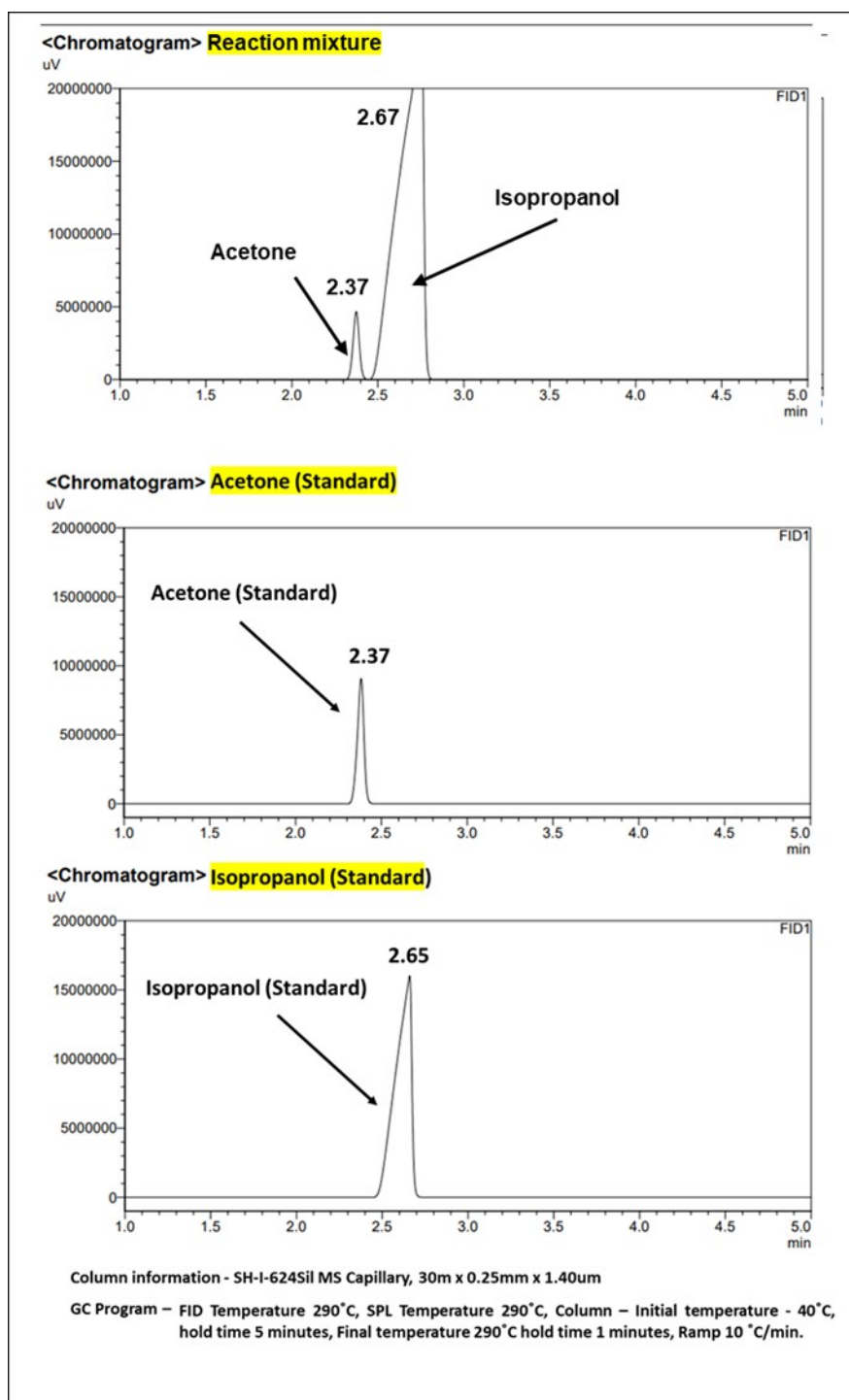


Fig. S9: GC chromatogram of the reaction mixture of BPE hydrogenolysis demonstrating the formation of acetone in the reaction. (Reaction conditions -light source (150 W LED),

photocatalyst 3%Pd@CN/rGO/BMO(2:1) (20 mg), reactant (0.1 mmol), IPA (5 ml)), H₂ (2 bar) time (3h).

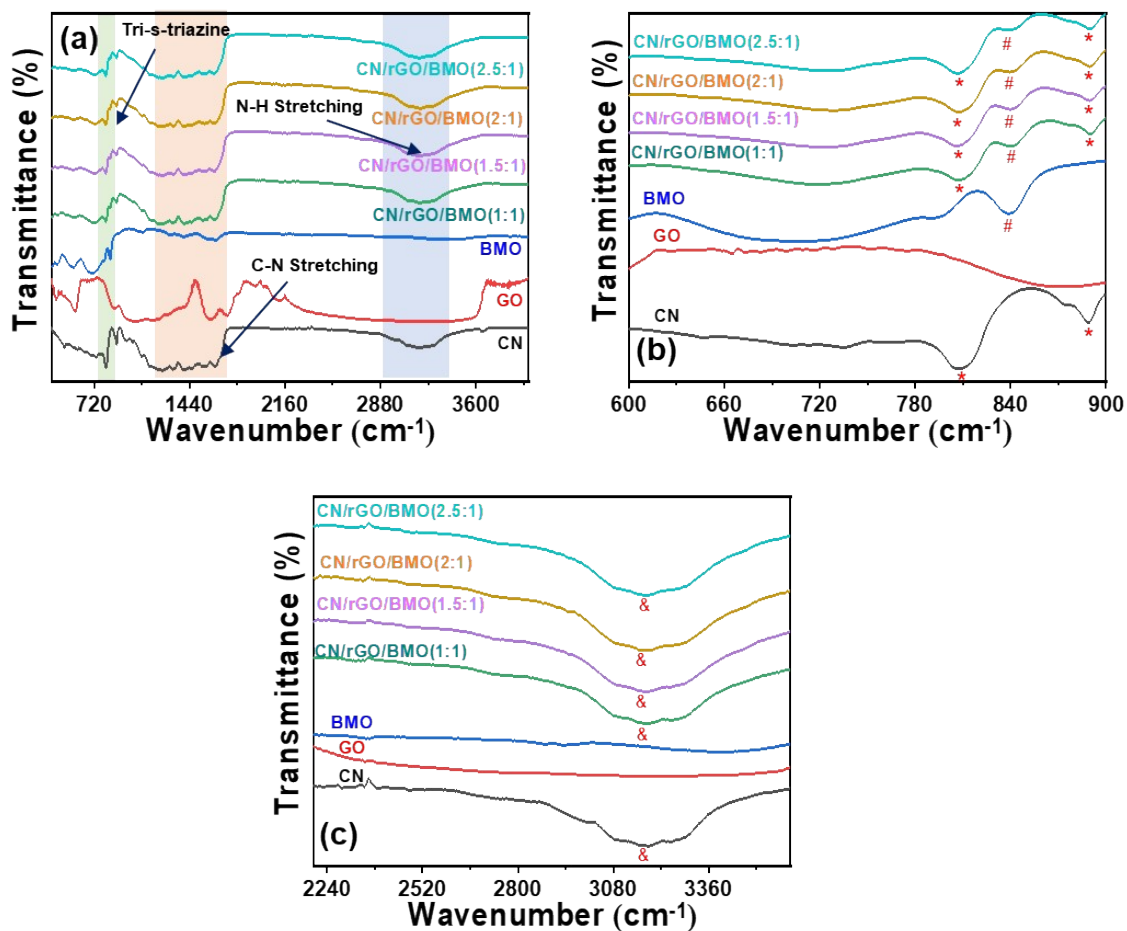


Fig. S10. (a) FTIR spectra of CN, GO, BMO, and the composite with various combinations of CN and BMO, and (b) & (c) Zoomed spectra clearly showing the characteristic peak of CN (* and &) and BMO (#).

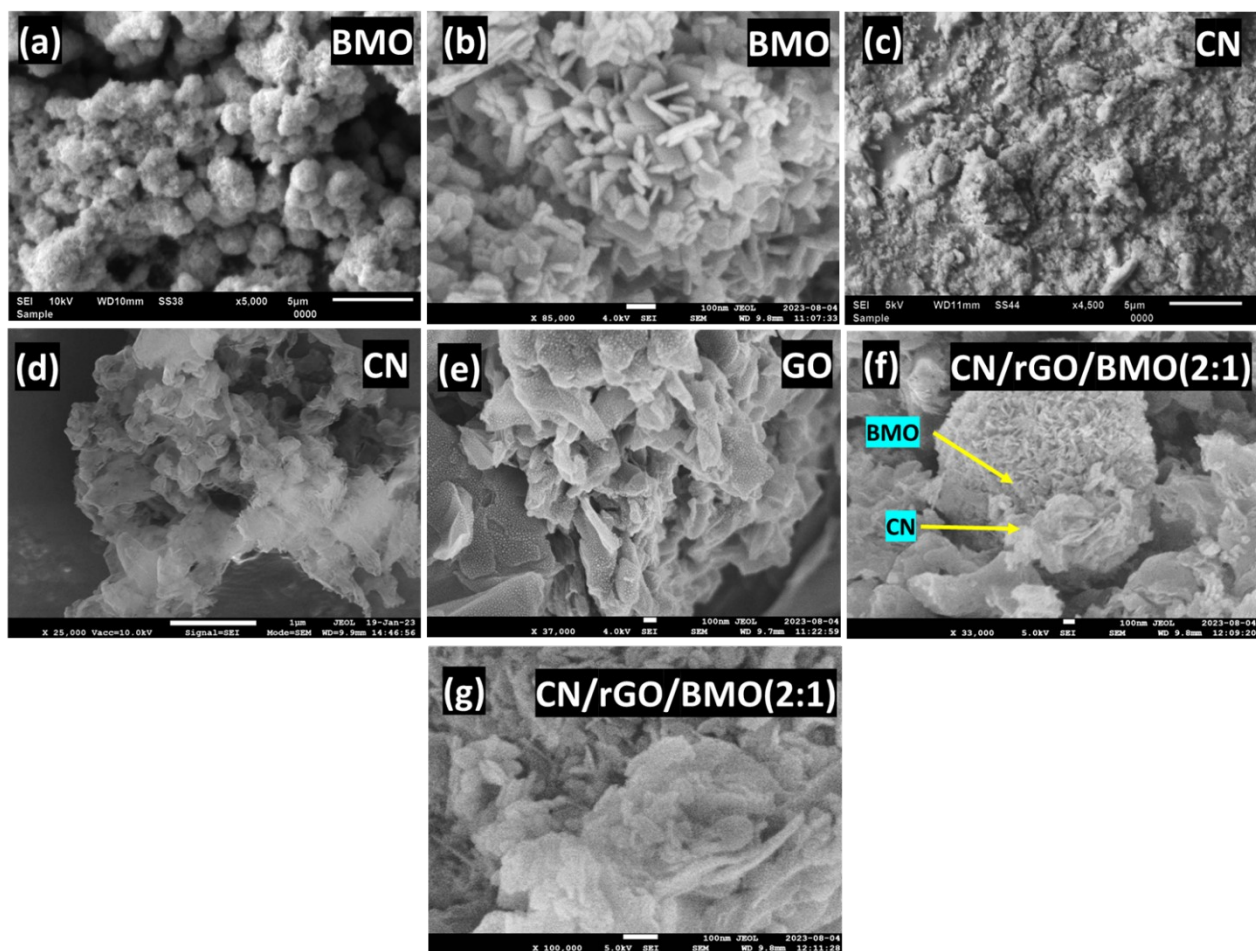


Fig. S11. SEM images of (a)-(b) BMO, (c)-(d) CN, (e) GO, and (f)-(g) CN/rGO/BMO.

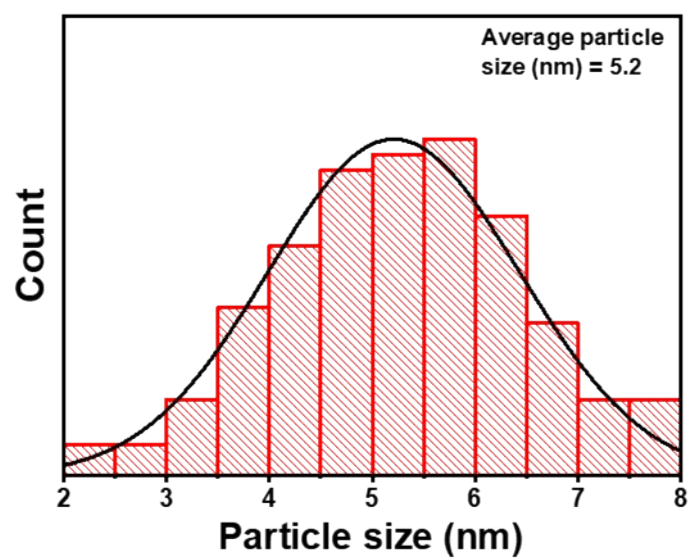


Fig. S12. Pd nanoparticles size distribution obtained from HR-TEM images of 3%Pd@CN/rGO/BMO(2:1).

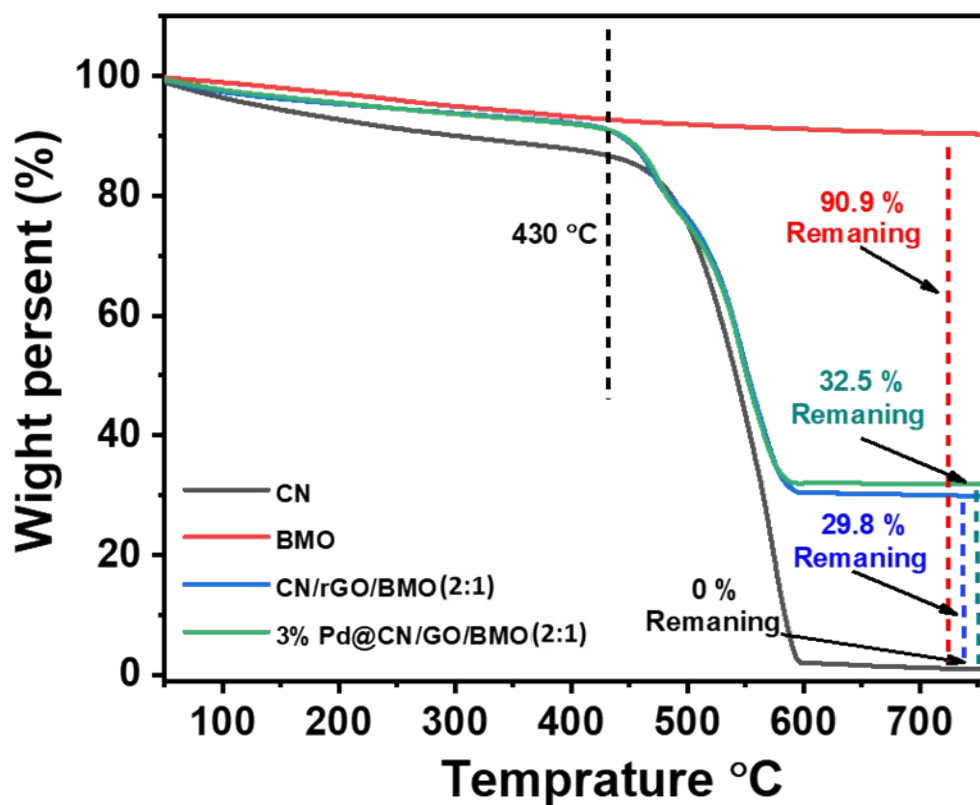


Fig. S13. Thermograms of the CN, BMO, CN/rGO/BMO(2:1), 3%Pd@CN/rGO/BMO(2:1) performed in N₂ gas.

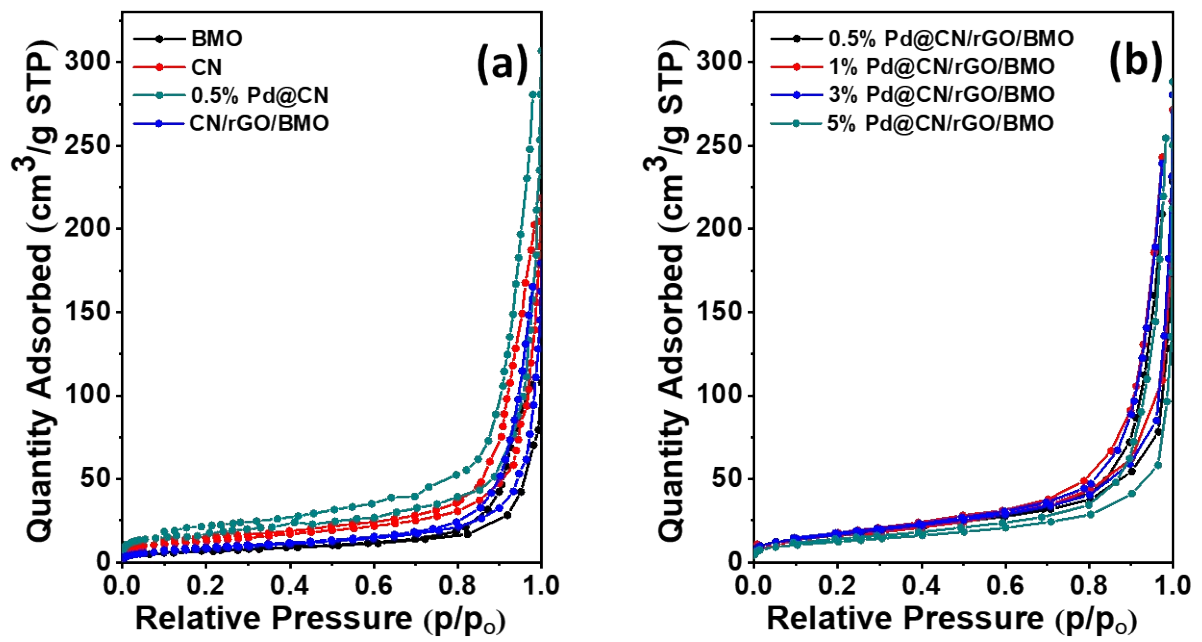


Fig. S14. N₂-adsorption/desorption isotherms of (a) BMO, CN, 0.5%Pd@CN and CN/rGO/BMO(2:1), and (b) 0.5%Pd@CN/rGO/BMO(2:1), 1%Pd@CN/rGO/BMO(2:1), 3%Pd@CN/rGO/BMO(2:1), and 5%Pd@CN/rGO/BMO(2:1).

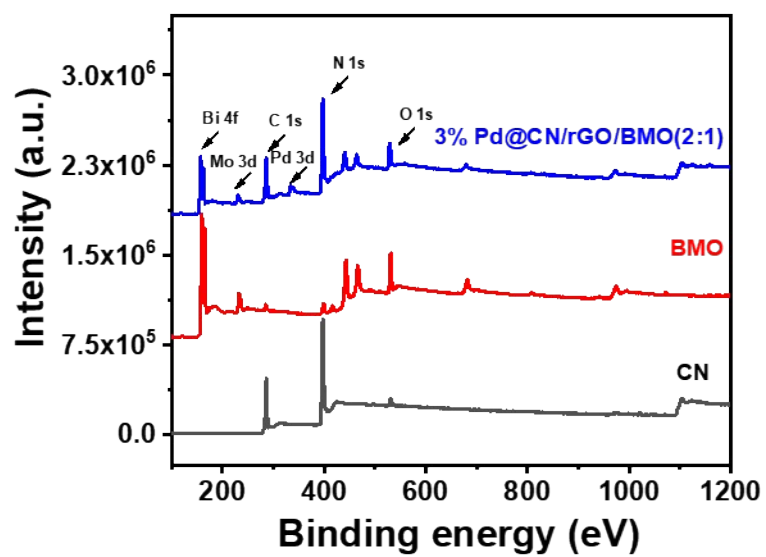


Fig. S15. XPS survey spectra of the photocatalysts (CN, BMO, and 3%Pd@CN/rGO/BMO(2:1)).

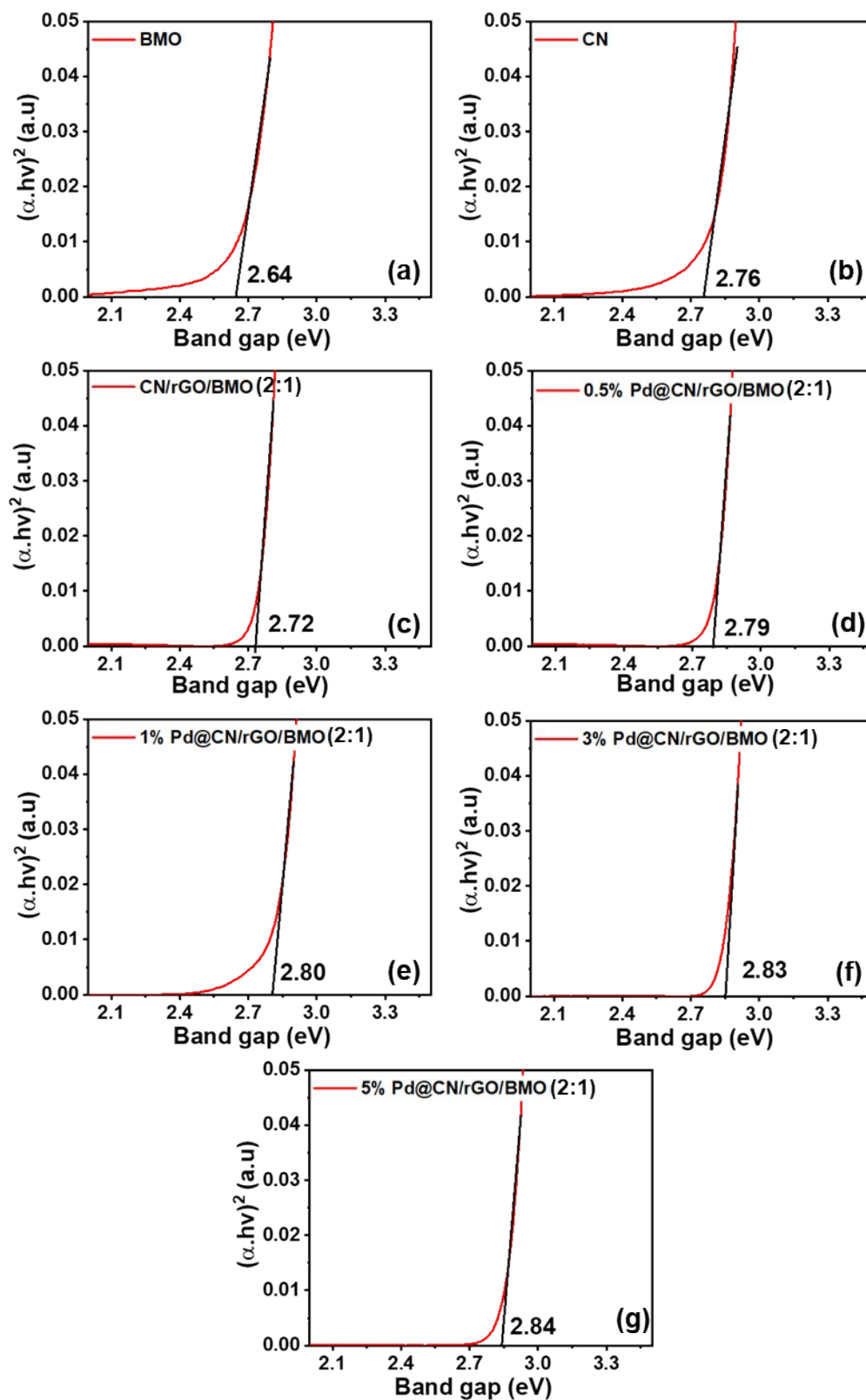


Fig. S16. Tauc plots (a-e) of synthesized photocatalysts.

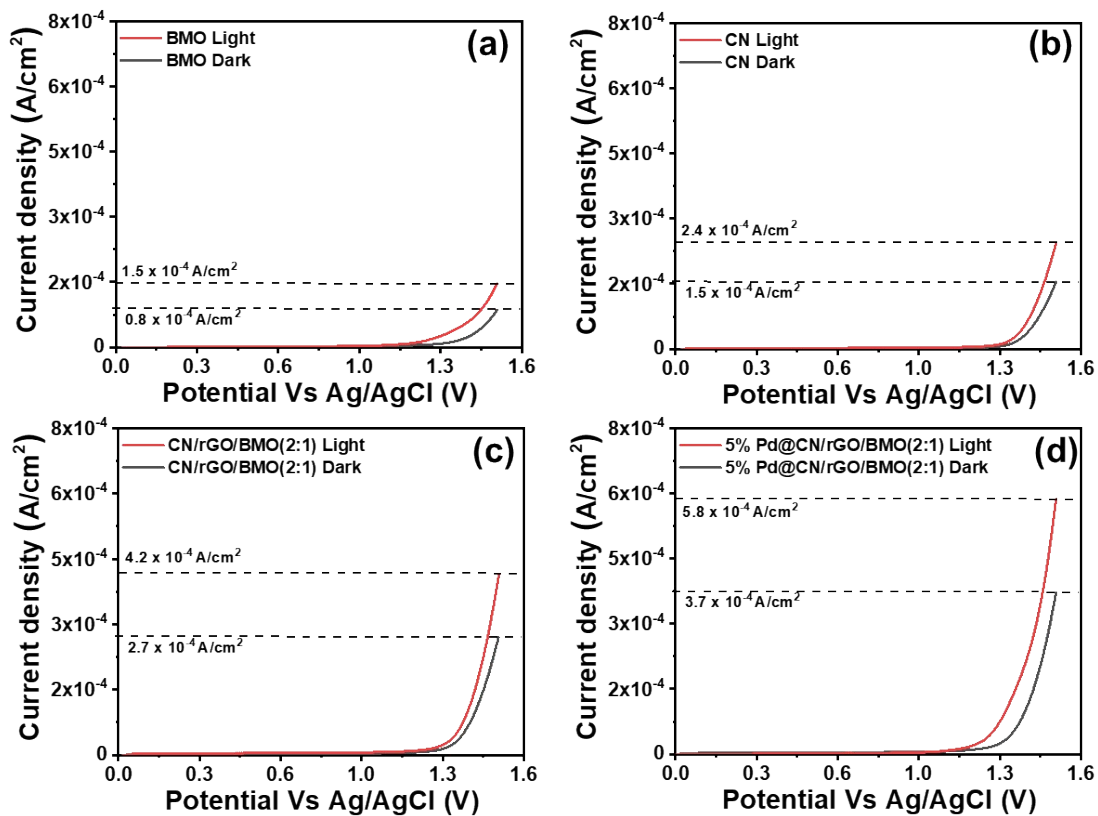


Fig. S17. LSV spectra of photocatalyst in dark and light for (a) BMO, (b) CN, (c) CN/rGO/BMO(2:1) composites, and (d) 5%Pd@CN/rGO/BMO(2:1).

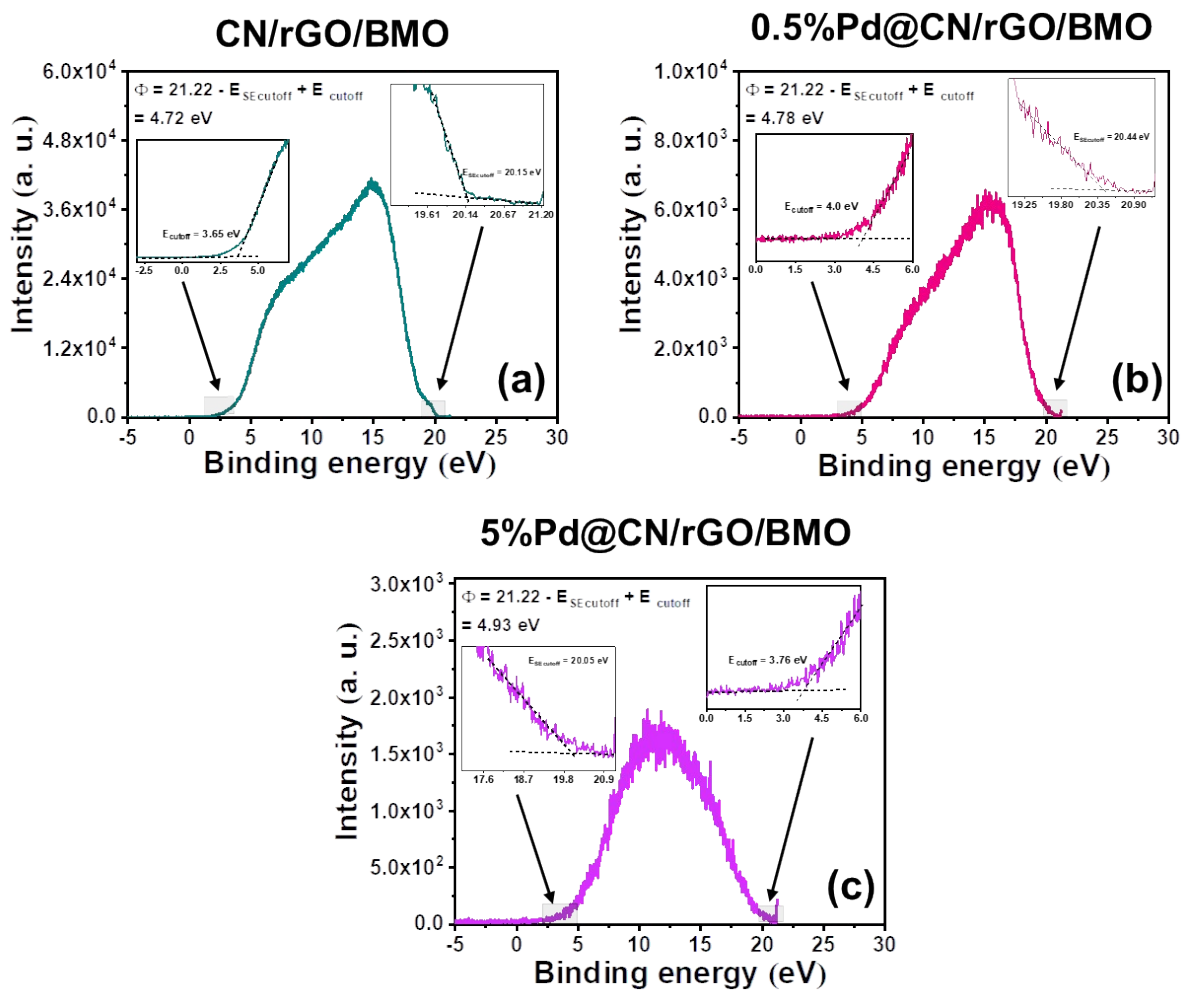


Fig. S18. UPS spectra of (a) CN/rGO/BMO, (b) 0.5%Pd@CN/rGO/BMO, and, (c) 5%Pd@CN/rGO/BMO.

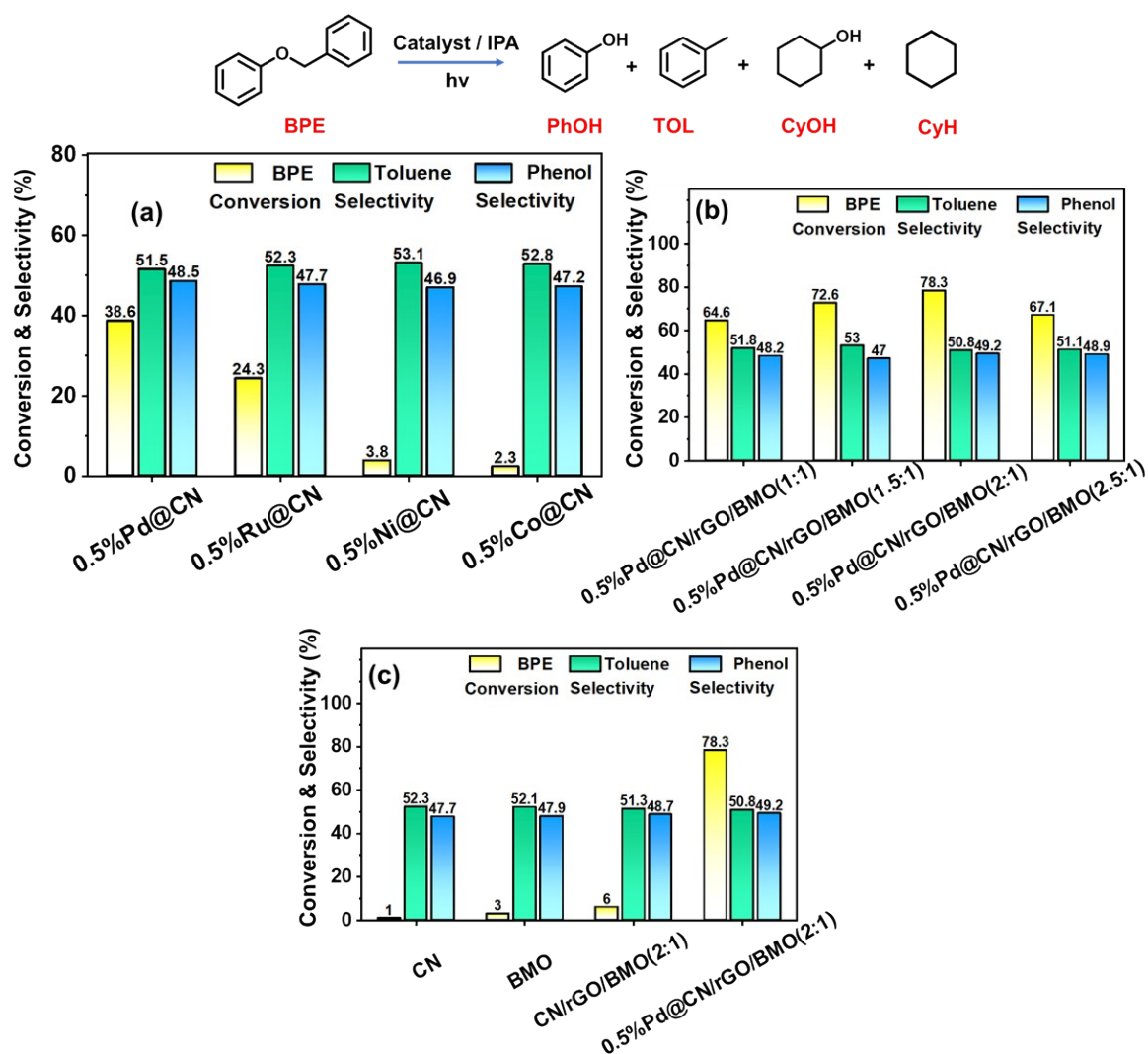


Fig. S19. BPE hydrogenolysis (a) catalyst with different metal NPs over CN (b) 0.5 % Pd over different variation of heterojunction (d) with individual component (CN, BMO, and CN/rGO/BMO) of heterojunction 3%Pd@CN/rGO/BMO. (Reaction conditions: light source (150 W LED), catalyst amount (20 mg), BPE (0.1 mmol)), H₂ (2 bar), time 3h, and IPA (5 ml).

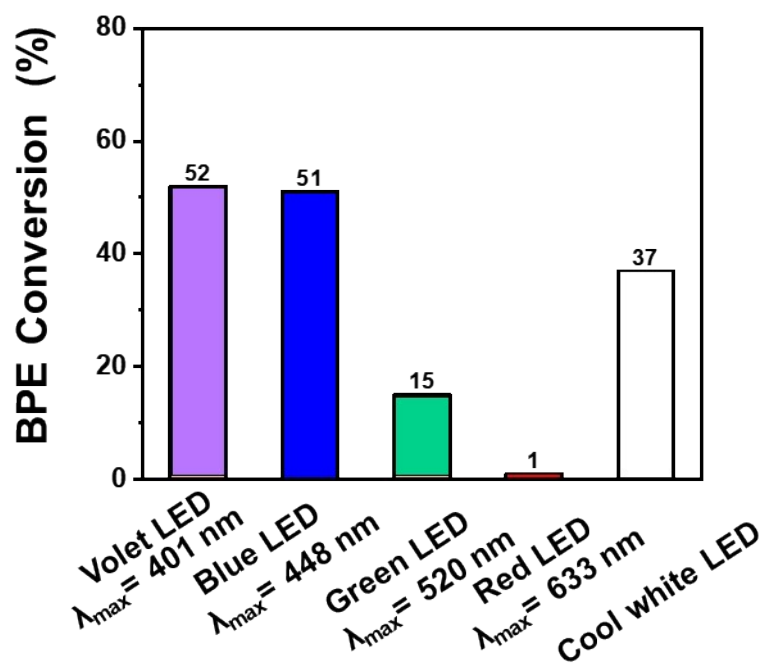


Fig. S20. Spectral response of 3%Pd@CN/rGO/BMO in different LEDs. (Reaction conditions: substrate (0.1 mmol), catalyst amount (20 mg), IPA (5 mL), 9W LEDs, room temperature, H₂ (2 bar), time (6 h).

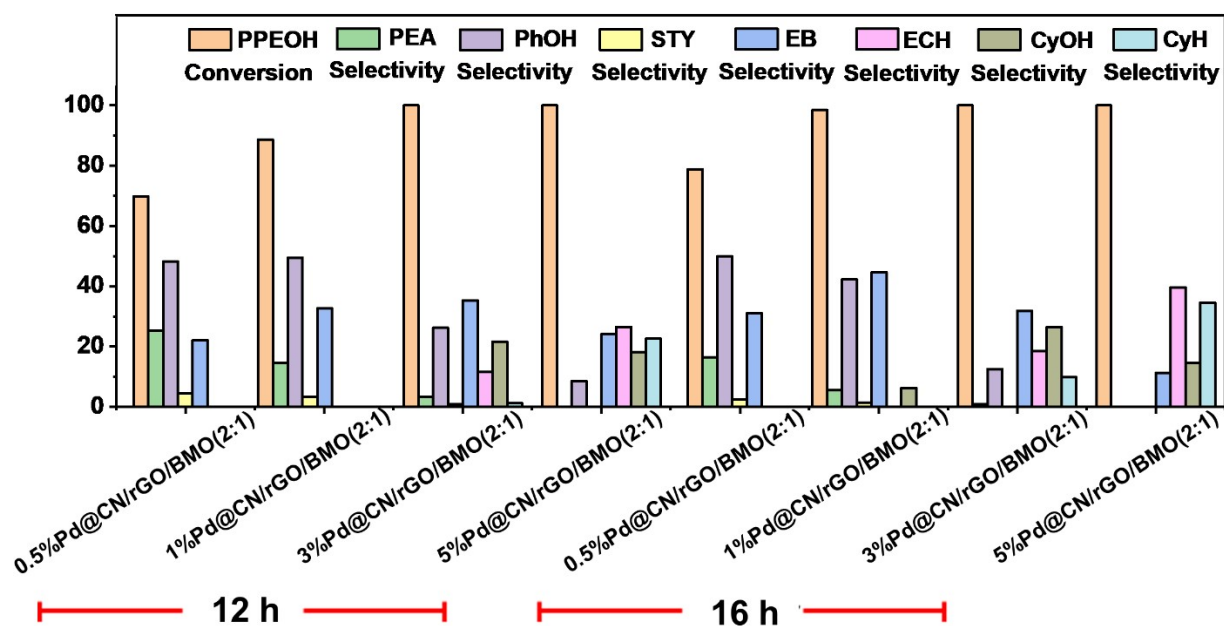
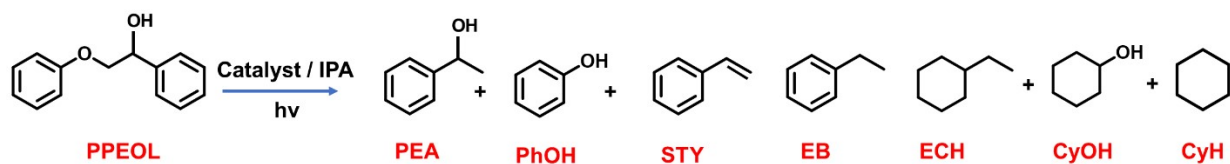


Fig. S21. PPEOL hydrogenolysis was conducted with different catalyst and time intervals. (Reaction conditions: light source (150 W LED), catalyst amount (20 mg), PPEOL (0.1 mmol), H₂ (2 bar), and IPA (5 ml)).

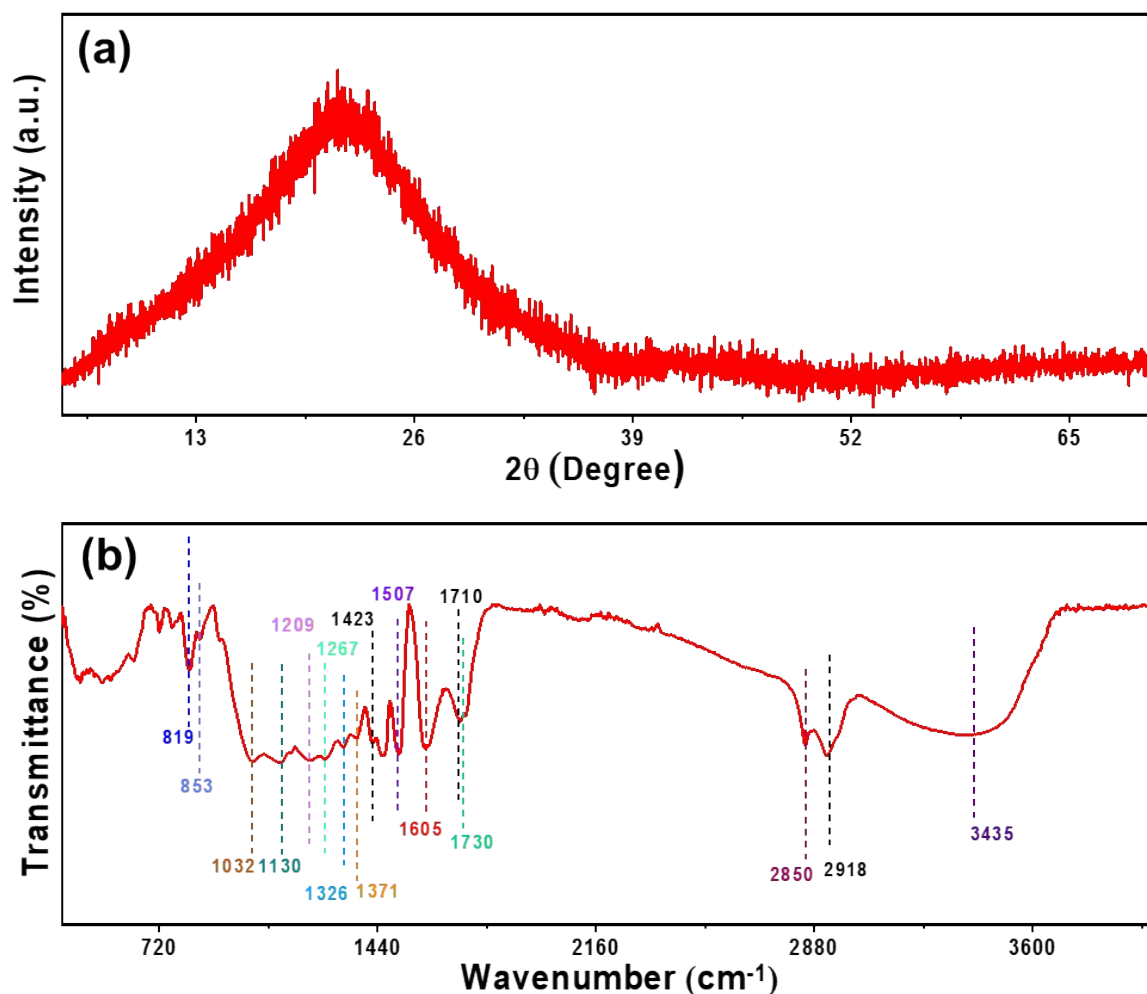


Fig. S22 (a) XRD pattern of extracted lignin, and (b) FTIR spectrum of extracted lignin.

In the extracted lignin, no impurity peaks corresponding to the cellulosic part ($\sim 19.8^\circ$, $\sim 22.5^\circ$ for crystalline, and $\sim 16.0^\circ$, $\sim 18.0^\circ$ for amorphous) were observed.^{S13,S14} Analysis of the XRD patterns revealed the complete disappearance of cellulose peaks, providing definitive evidence for the purity of the extracted lignin.^{S15}

The FT-IR spectra were analyzed to identify the functional groups in the extracted lignin. Based on previous literature,^{S16-S18} the main peaks of lignin in FT-IR spectra were assigned. The broad peak at 3435 cm^{-1} is assigned to the stretching vibrations of O–H groups. The peaks at 2918 cm^{-1} and 2850 cm^{-1} are assigned to the anti-symmetric stretching and stretching in methylene groups, respectively. The peaks at 1730 cm^{-1} to 1710 cm^{-1} are attributed to the C=O stretching vibration of unconjugated carbonyl groups, and the peaks at 1605 cm^{-1} , 1507 cm^{-1} , and 1423 cm^{-1} are attributed to characteristic vibrations from aromatic rings. The spectra of all lignin samples showed vibrations characteristic of the guaiacyl unit (1267 cm^{-1} , G ring and C=O

stretch; 1130 cm^{-1} , CH in-plane deformation; 853 and 819 cm^{-1} , C–H out-of-plane vibrations in positions 2, 5, and 6 of guaiacyl units), but the intensity of the bands varied significantly between samples. Moreover, lignin showed a band at 1326 cm^{-1} , which is characteristic of syringyl (S) ring plus guaiacyl (G) ring condensed, and the vibration at 843 cm^{-1} , which arises from the C–H out-of-plane in positions 2 and 6 of S units. A weak band at 1371 cm^{-1} originated from phenolic OH and aliphatic C–H in methyl groups, and a strong vibration at 1209 cm^{-1} could be associated with C–C plus C–O plus C=O stretching. The aromatic C–H deformation at 1032 cm^{-1} appeared as a complex vibration associated with the C–O, C–C stretching, and C–OH bending in polysaccharides.

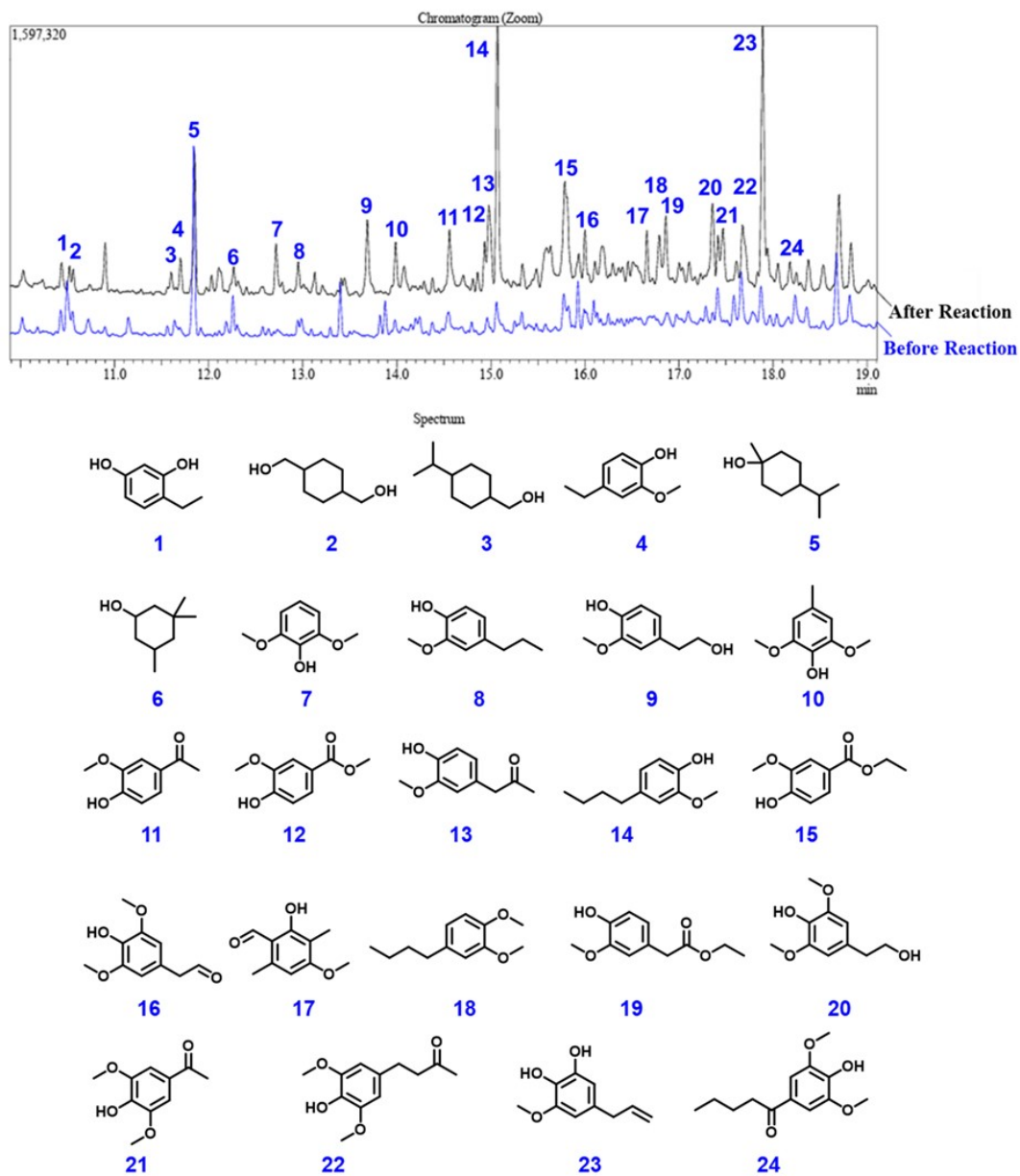
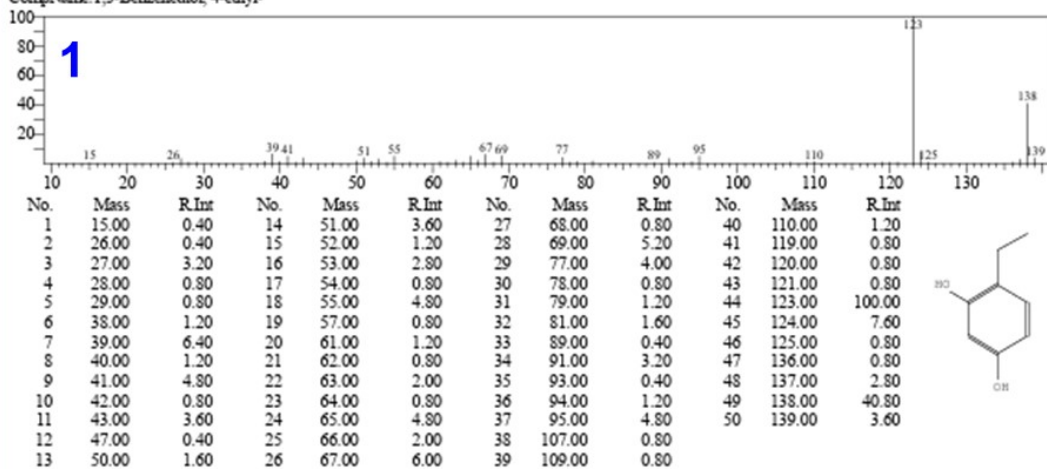


Fig. S23 GC-MS chromatograph of lignin-MeOH solution before and after photocatalysis.

(Reaction conditions -light source (150 W LED), photocatalyst 5%Pd@CN/rGO/BMO(2:1) (50 mg), (extracted lignin 300 mg, MeOH 10 ml), H₂ (5 bar) time (24 h)).

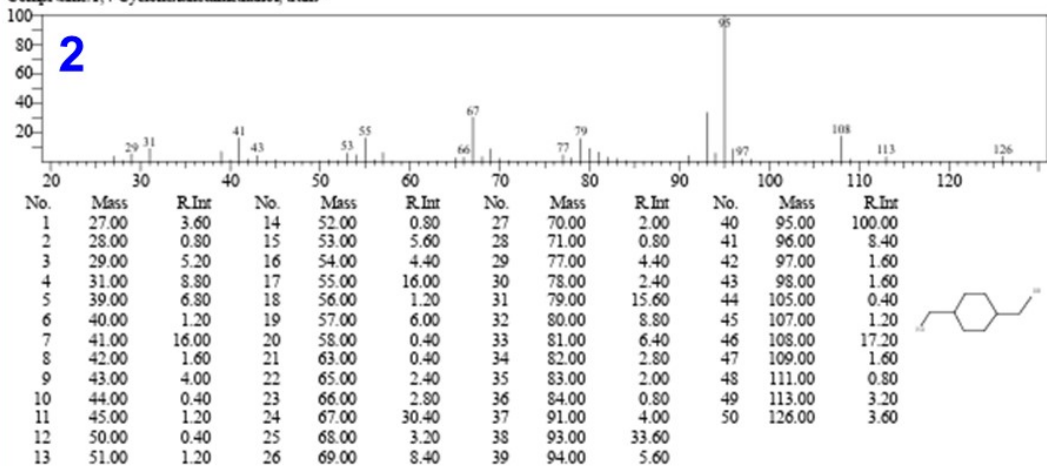
Compound Information

Entry:19215 Library:NIST17.LIB
 Formula:C8H10O2 CAS:2896-60-8 MolWeight:138 RetIndex:1334
 CompName:1,3-Benzenediol, 4-ethyl-



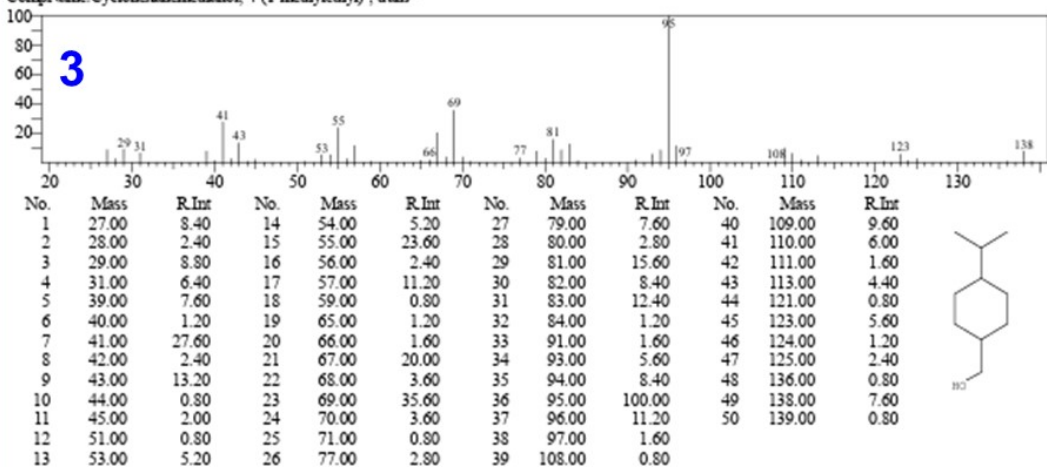
Compound Information

Entry:23434 Library:NIST17.LIB
 Formula:C8H16O2 CAS:3236-48-4 MolWeight:144 RetIndex:1327
 CompName:1,4-Cyclohexanedimethanol, trans-



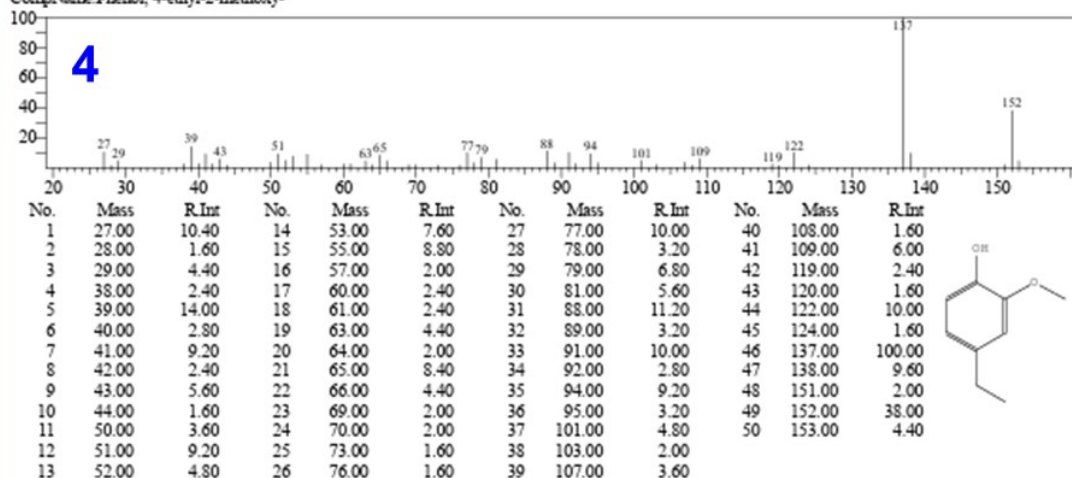
Compound Information

Entry:32467 Library:NIST17.LIB
 Formula:C10H20O CAS:13674-19-6 MolWeight:156 RetIndex:1219
 CompName:Cyclohexanemethanol, 4-(1-methylethyl)-, trans-



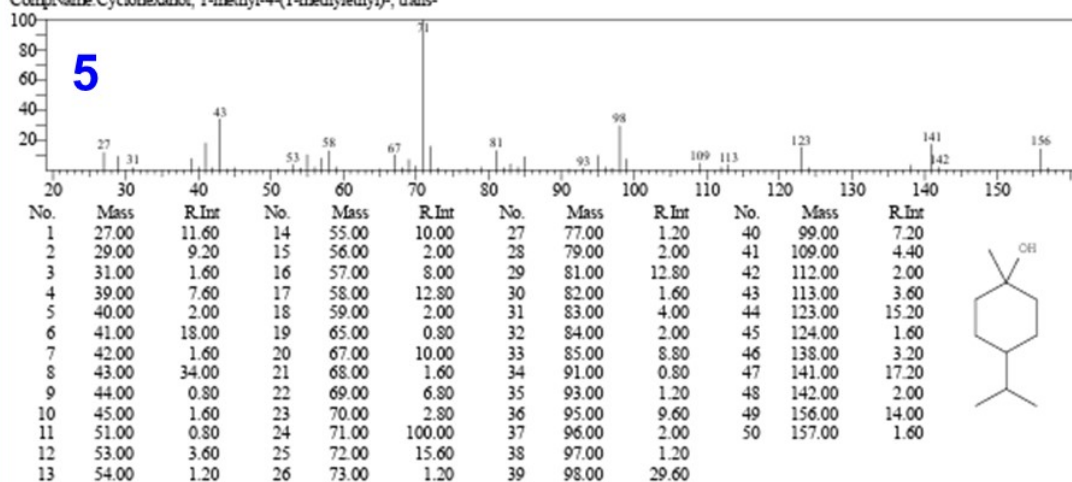
Compound Information

Entry:28683 Library:NIST17.LIB
 Formula:C9H12O2 CAS:2785-89-9 MolWeight:152 RetIndex:1303
 CompName:Phenol, 4-ethyl-2-methoxy-



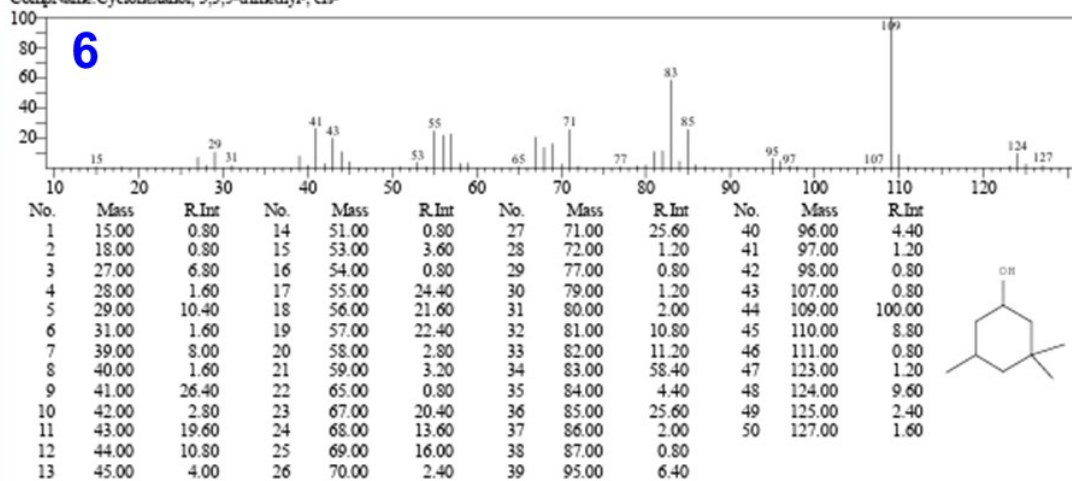
Compound Information

Entry:32440 Library:NIST17.LIB
 Formula:C10H20O CAS:3901-93-7 MolWeight:156 RetIndex:1127
 CompName:Cyclohexanol, 1-methyl-4-(1-methylethyl)-, trans-



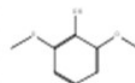
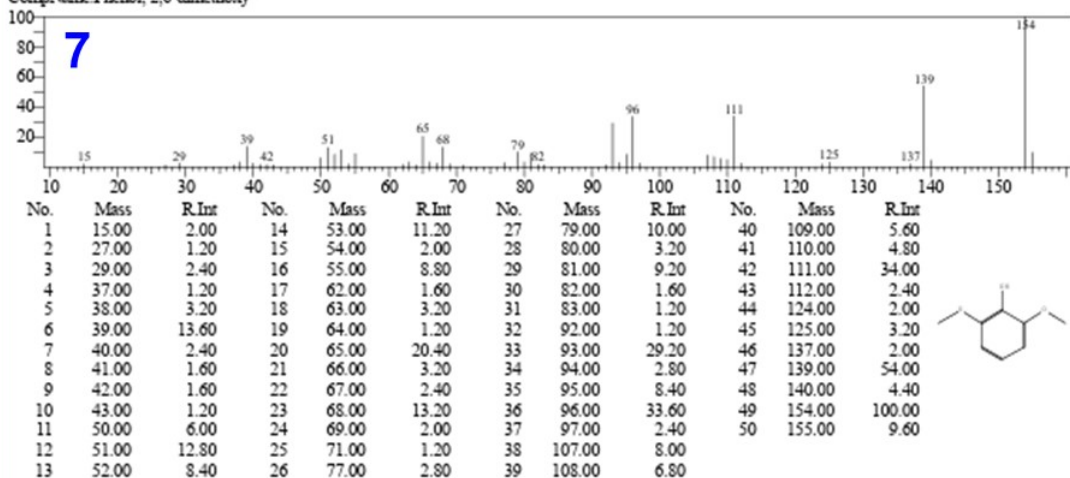
Compound Information

Entry:22225 Library:NIST17.LIB
 Formula:C9H18O CAS:933-48-2 MolWeight:142 RetIndex:1103
 CompName:Cyclohexanol, 3,3,5-trimethyl-, cis-



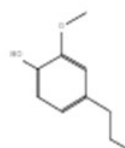
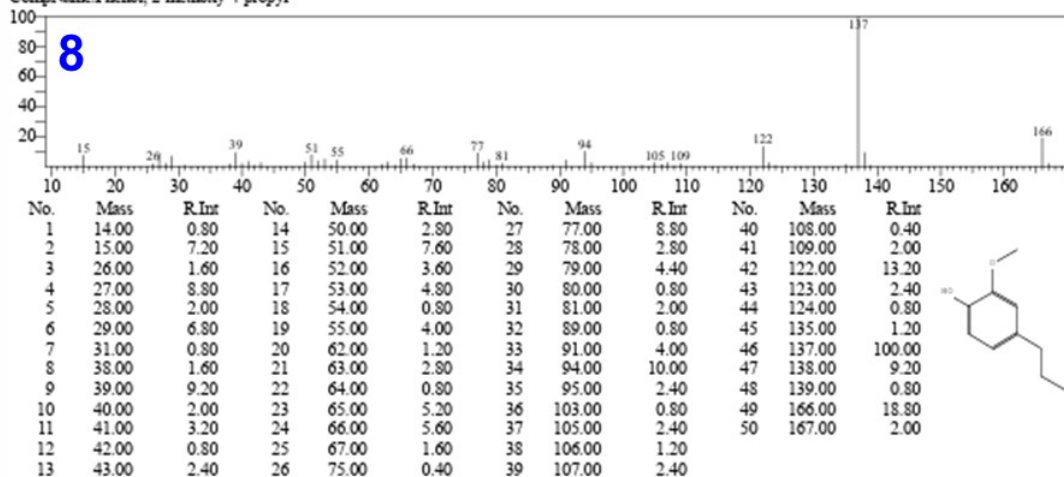
Compound Information

Entry:30198 Library:NIST17.LIB
 Formula:C8H10O3 CAS:91-10-1 MolWeight:154 RetIndex:1279
 CompName:Phenol, 2,6-dimethoxy-



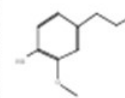
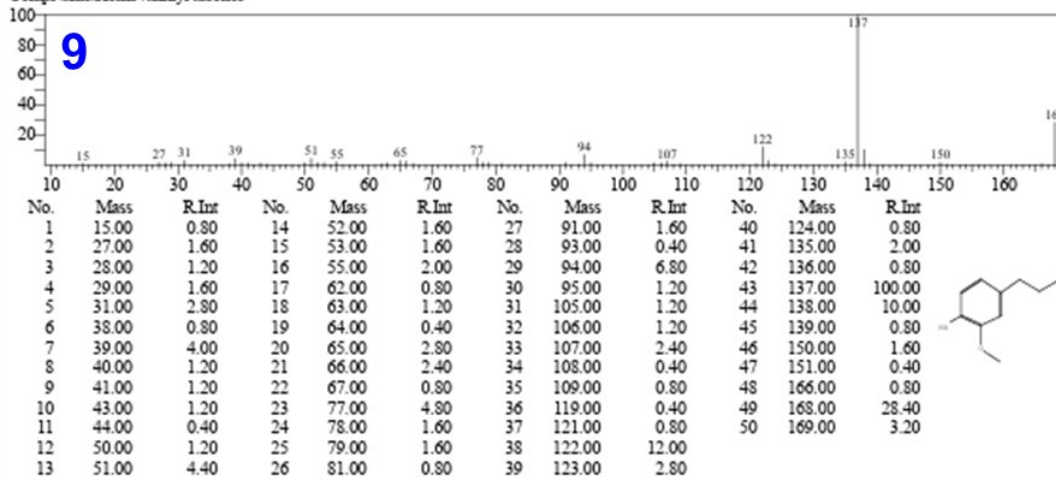
Compound Information

Entry:40071 Library:NIST17.LIB
 Formula:C10H14O2 CAS:2785-87-7 MolWeight:166 RetIndex:1402
 CompName:Phenol, 2-methoxy-4-propyl-



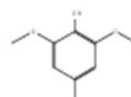
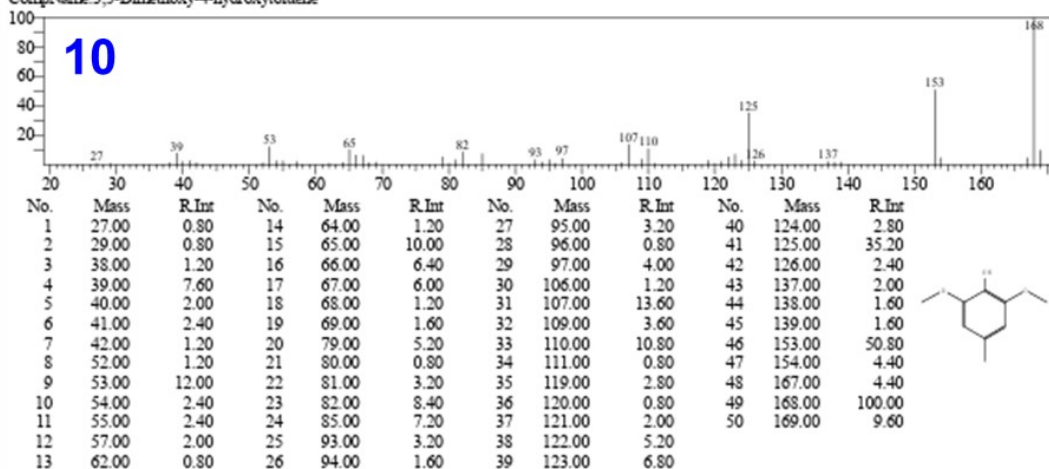
Compound Information

Entry:41482 Library:NIST17.LIB
 Formula:C9H12O3 CAS:2380-78-1 MolWeight:168 RetIndex:1545
 CompName:Homovanillyl alcohol



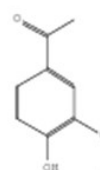
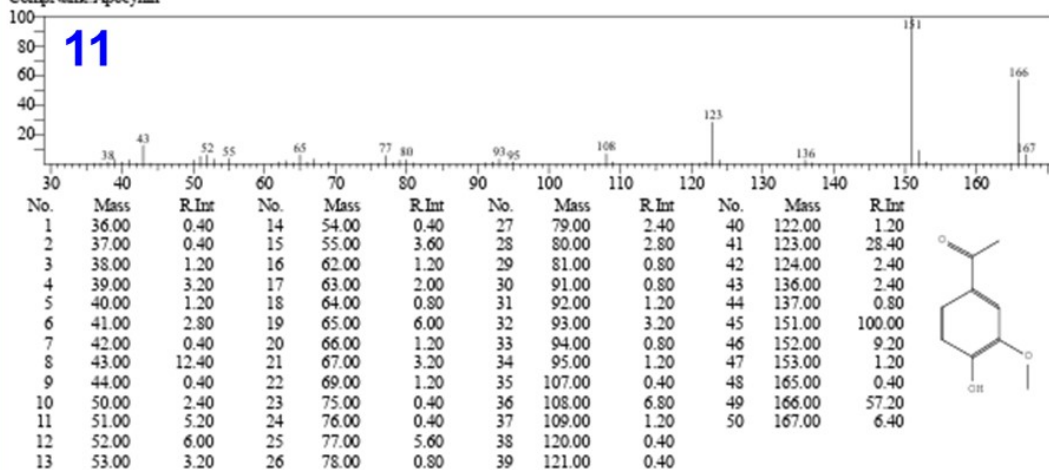
Compound Information

Entry:41498 Library:NIST17.LIB
 Formula:C9H12O3 CAS:6638-05-7 MolWeight:168 RetIndex:1392
 CompName:3,5-Dimethoxy-4-hydroxytoluene



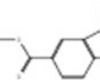
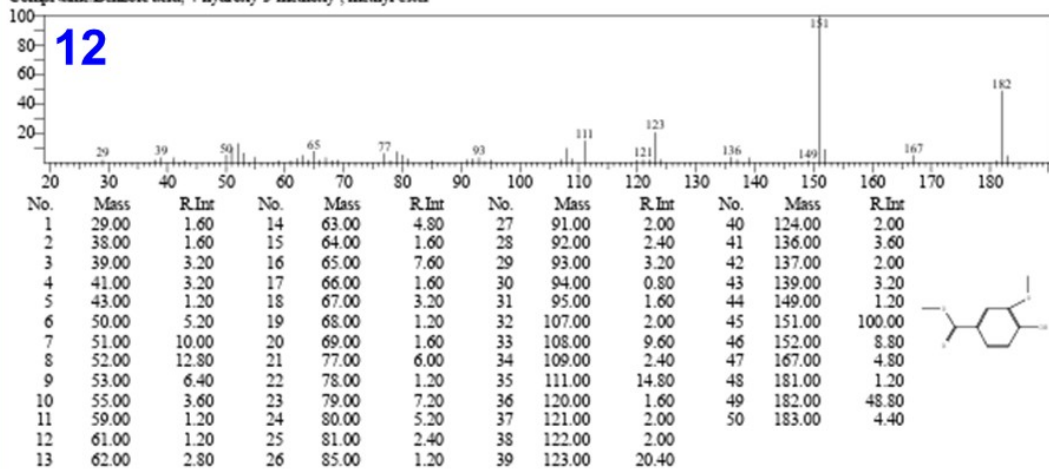
Compound Information

Entry:39837 Library:NIST17.LIB
 Formula:C9H10O3 CAS:498-02-2 MolWeight:166 RetIndex:1439
 CompName:Apocynin



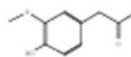
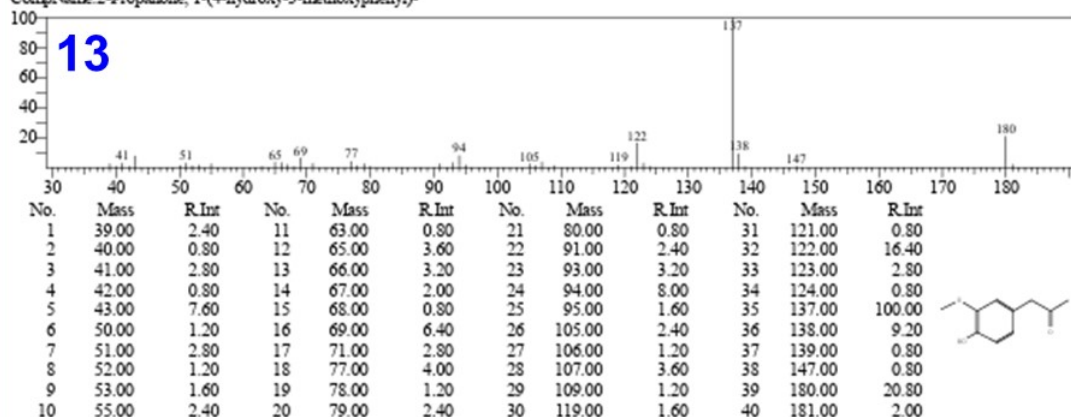
Compound Information

Entry:53865 Library:NIST17.LIB
 Formula:C9H10O4 CAS:3943-74-6 MolWeight:182 RetIndex:1470
 CompName:Benzoic acid, 4-hydroxy-3-methoxy-, methyl ester



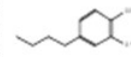
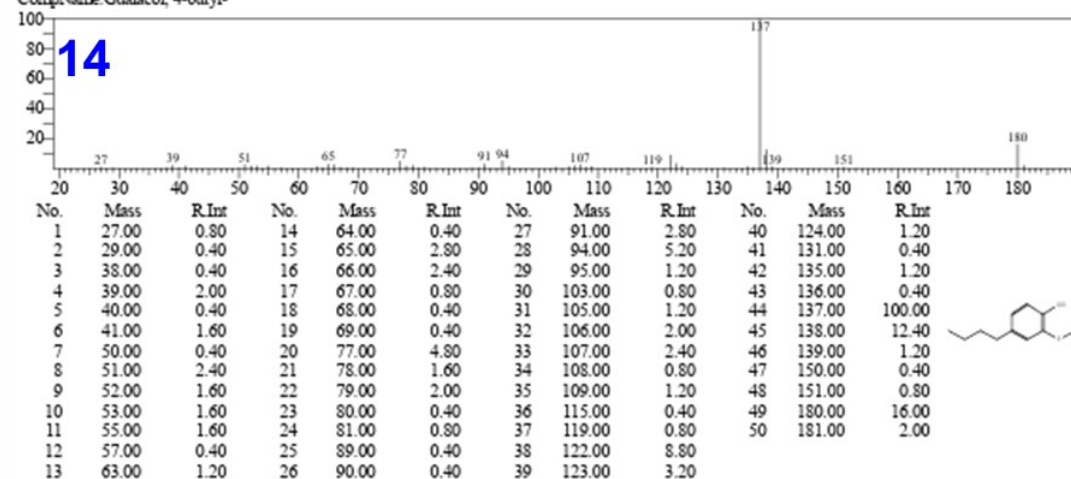
Compound Information

Entry:52209 Library:NIST17.LIB
 Formula:C10H12O3 CAS:2503-46-0 MolWeight:180 RetIndex:1538
 CompName:2-Propanone, 1-(4-hydroxy-3-methoxyphenyl)-



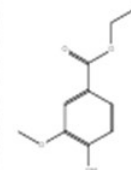
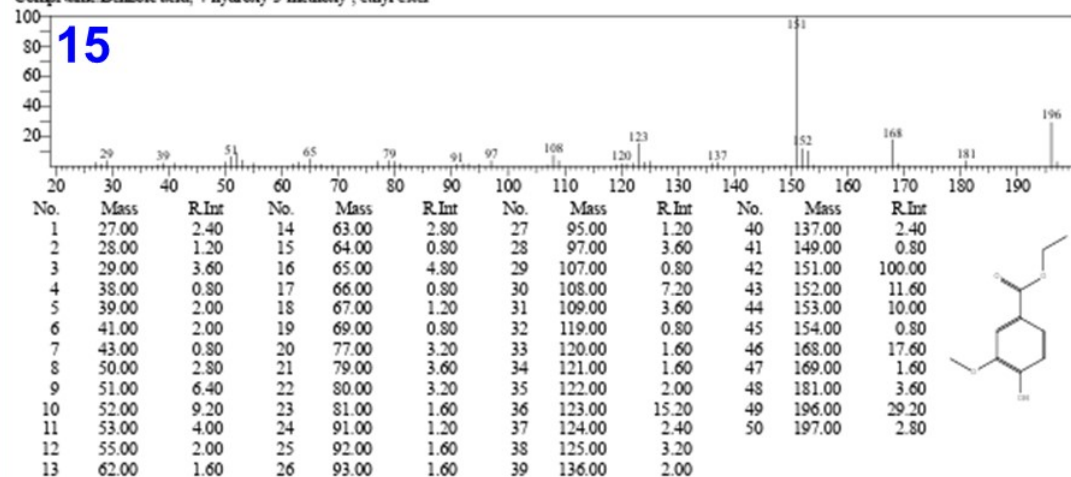
Compound Information

Entry:52404 Library:NIST17.LIB
 Formula:C11H16O2 CAS:59832-96-1 MolWeight:180 RetIndex:1502
 CompName:Guaiacol, 4-butyl-



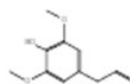
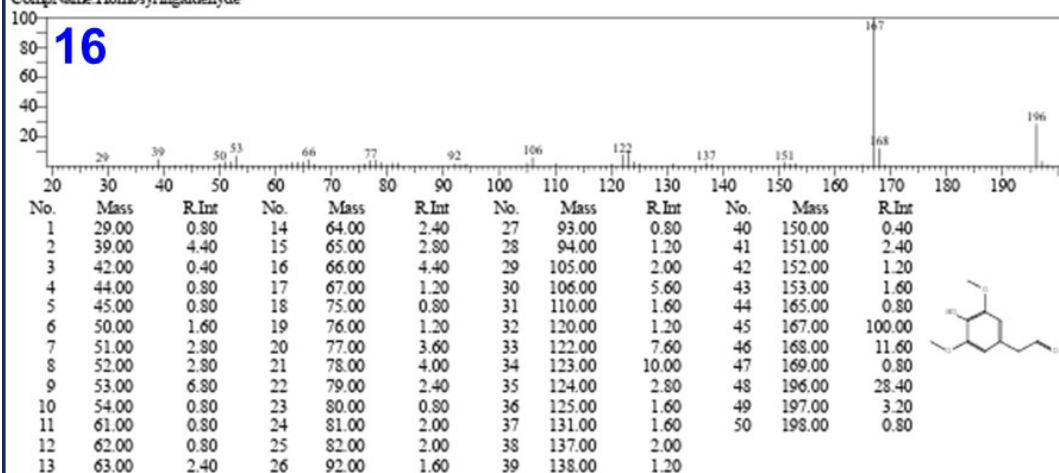
Compound Information

Entry:66947 Library:NIST17.LIB
 Formula:C10H12O4 CAS:617-05-0 MolWeight:196 RetIndex:1569
 CompName:Benzoic acid, 4-hydroxy-3-methoxy-, ethyl ester



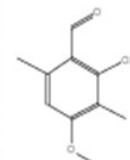
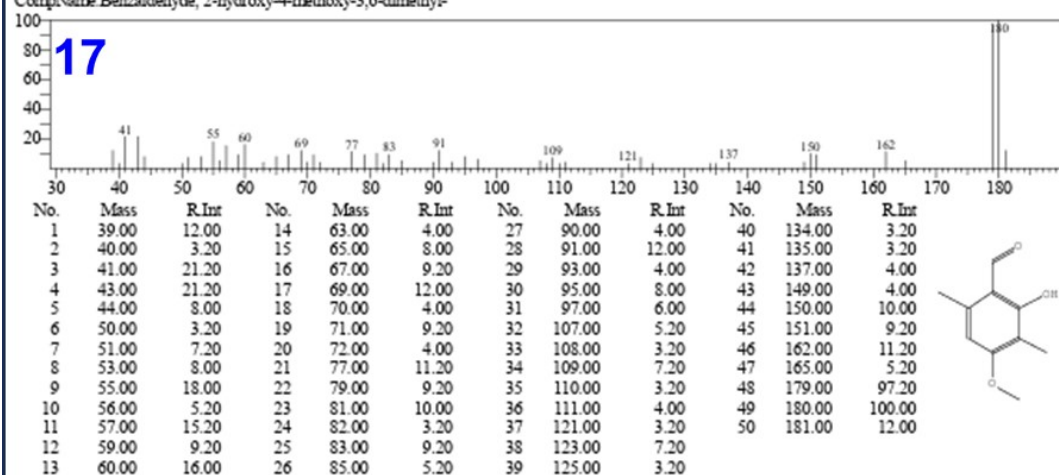
Compound Information

Entry:66902 Library:NIST17.LIB
 Formula:C10H12O4 CAS:37345-52-6 MolWeight:196 RefIndex:1630
 CompName:Homosyringaldehyde



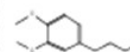
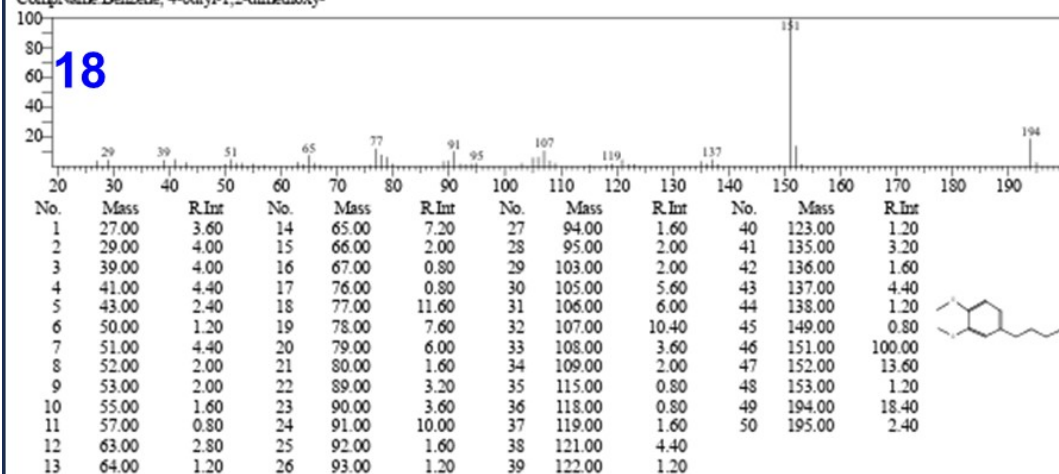
Compound Information

Entry:52144 Library:NIST17.LIB
 Formula:C10H12O5 CAS:34883-15-3 MolWeight:180 RefIndex:1618
 CompName: Benzaldehyde, 2-hydroxy-4-methoxy-3,6-dimethyl-



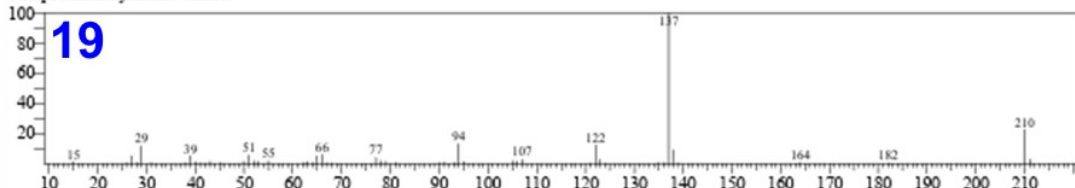
Compound Information

Entry:65340 Library:NIST17.LIB
 Formula:C12H18O2 CAS:59056-76-7 MolWeight:194 RefIndex:1470
 CompName: Benzene, 4-butyl-1,2-dimethoxy-

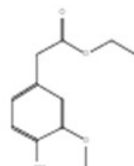


Compound Information

Entry:80993 Library:NIST17.LIB
 Formula:C11H14O4 CAS:60563-13-5 MolWeight:210 RetIndex:1669
 CompName:Ethyl homovanillate

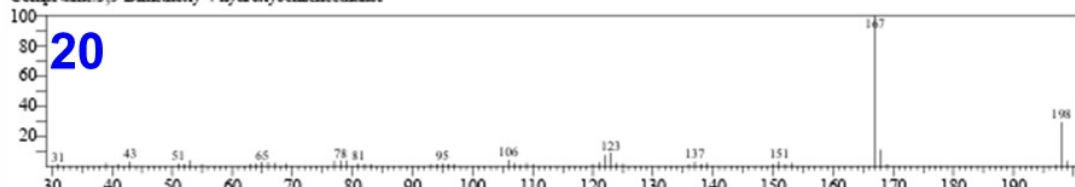


No.	Mass	R.Int	No.	Mass	R.Int	No.	Mass	R.Int	No.	Mass	R.Int
1	15.00	1.20	14	50.00	1.60	27	78.00	2.00	40	123.00	2.80
2	26.00	0.80	15	51.00	5.60	28	79.00	1.60	41	124.00	0.40
3	27.00	5.20	16	52.00	2.00	29	81.00	0.80	42	135.00	0.80
4	28.00	0.80	17	53.00	1.60	30	90.00	0.80	43	136.00	0.80
5	29.00	11.60	18	55.00	2.00	31	91.00	1.20	44	137.00	100.00
6	31.00	0.80	19	62.00	0.80	32	93.00	0.80	45	138.00	9.20
7	38.00	0.80	20	63.00	1.20	33	94.00	13.20	46	139.00	0.80
8	39.00	5.20	21	64.00	0.80	34	95.00	1.20	47	164.00	0.80
9	40.00	1.20	22	65.00	5.20	35	105.00	2.00	48	182.00	0.40
10	41.00	0.80	23	66.00	6.00	36	106.00	1.60	49	210.00	22.40
11	42.00	0.40	24	67.00	0.80	37	107.00	2.80	50	211.00	2.80
12	43.00	1.60	25	68.00	0.40	38	121.00	0.40			
13	45.00	0.80	26	77.00	4.00	39	122.00	12.40			

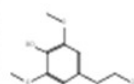


Compound Information

Entry:68916 Library:NIST17.LIB
 Formula:C10H14O4 CAS:20824-45-7 MolWeight:198 RetIndex:1735
 CompName:3,5-Dimethoxy-4-hydroxybenzeneethanol

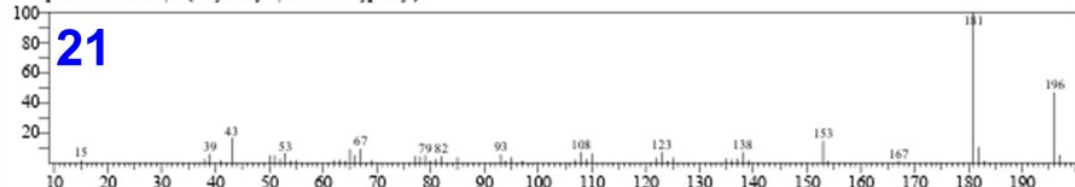


No.	Mass	R.Int	No.	Mass	R.Int	No.	Mass	R.Int	No.	Mass	R.Int
1	31.00	1.20	14	69.00	1.60	27	107.00	2.00	40	139.00	2.00
2	39.00	2.00	15	77.00	3.20	28	108.00	0.80	41	150.00	1.20
3	41.00	1.20	16	78.00	3.60	29	109.00	2.00	42	151.00	2.80
4	43.00	2.80	17	79.00	3.60	30	110.00	1.20	43	152.00	1.20
5	51.00	1.60	18	81.00	1.60	31	120.00	1.20	44	153.00	2.00
6	52.00	1.20	19	82.00	1.20	32	121.00	2.40	45	167.00	100.00
7	53.00	3.60	20	83.00	1.20	33	122.00	7.20	46	168.00	10.80
8	55.00	1.20	21	93.00	1.20	34	123.00	8.80	47	169.00	1.20
9	63.00	1.20	22	94.00	1.20	35	124.00	2.00	48	197.00	0.80
10	64.00	1.60	23	95.00	1.60	36	125.00	1.60	49	198.00	29.20
11	65.00	2.40	24	96.00	1.20	37	136.00	1.20	50	199.00	3.20
12	66.00	2.40	25	97.00	1.20	38	137.00	2.80			
13	67.00	2.00	26	106.00	4.00	39	138.00	1.20			

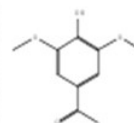


Compound Information

Entry:66963 Library:NIST17.LIB
 Formula:C10H12O4 CAS:2478-38-8 MolWeight:196 RetIndex:1628
 CompName:Ethaneone, 1-(4-hydroxy-3,5-dimethoxyphenyl)-



No.	Mass	R.Int	No.	Mass	R.Int	No.	Mass	R.Int	No.	Mass	R.Int
1	15.00	1.60	14	64.00	1.20	27	94.00	1.20	40	137.00	2.80
2	38.00	2.40	15	65.00	8.80	28	95.00	3.60	41	138.00	6.80
3	39.00	5.60	16	66.00	4.80	29	97.00	1.20	42	139.00	1.60
4	41.00	1.60	17	67.00	9.20	30	107.00	2.00	43	153.00	14.40
5	43.00	16.40	18	69.00	1.60	31	108.00	7.20	44	154.00	1.20
6	50.00	4.80	19	77.00	4.40	32	109.00	2.40	45	167.00	1.20
7	51.00	4.80	20	78.00	4.00	33	110.00	6.00	46	181.00	100.00
8	52.00	2.40	21	79.00	4.80	34	122.00	3.20	47	182.00	10.40
9	53.00	6.40	22	80.00	1.20	35	123.00	7.20	48	183.00	1.20
10	54.00	1.20	23	81.00	2.40	36	124.00	1.20	49	196.00	46.80
11	55.00	1.60	24	82.00	4.40	37	125.00	3.20	50	197.00	5.20
12	62.00	1.60	25	85.00	3.60	38	135.00	2.80			
13	63.00	2.00	26	93.00	5.60	39	136.00	2.00			



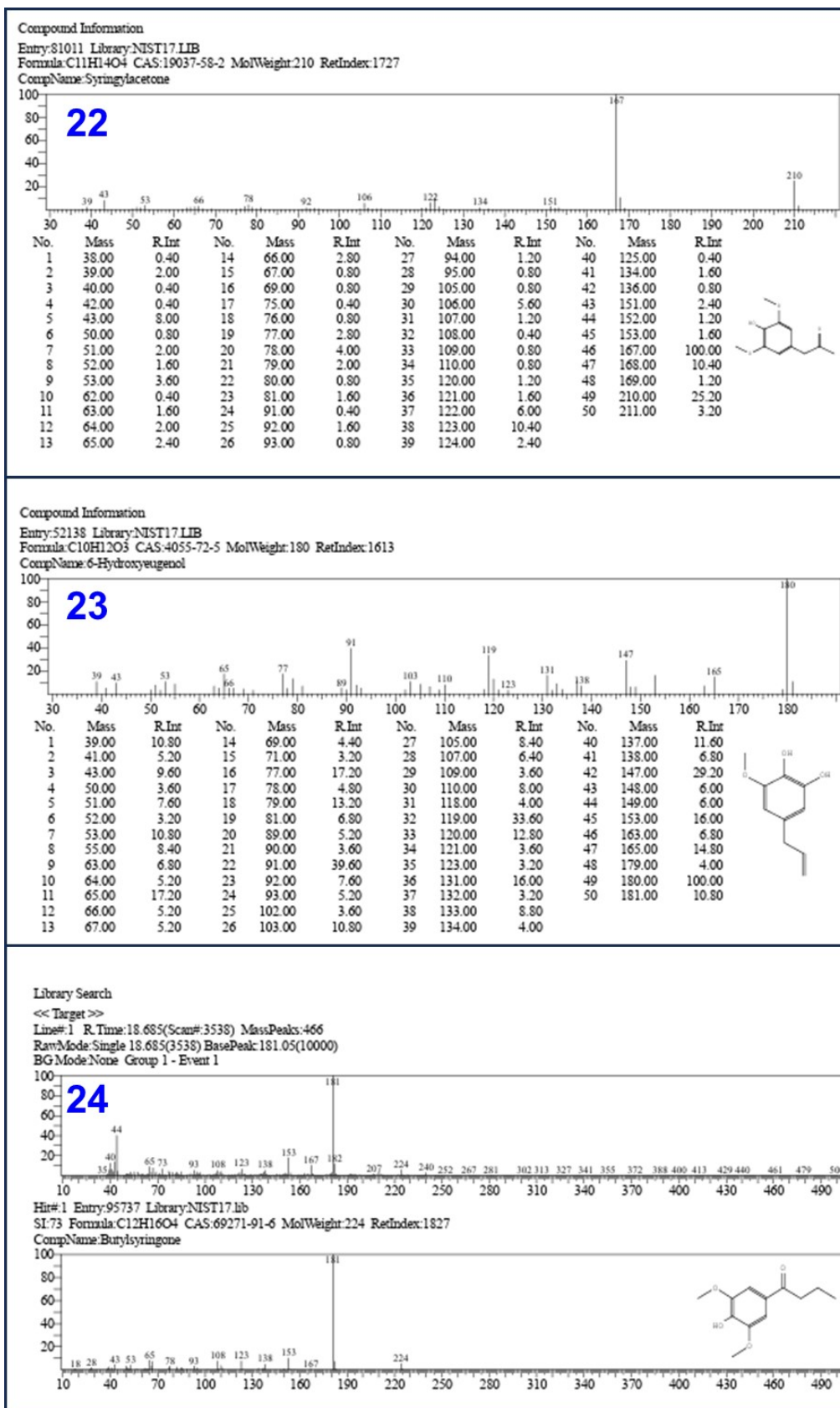


Fig. S24 MS spectra of the monomers (1 to 24) obtained after the photocatalytic process of real lignin.

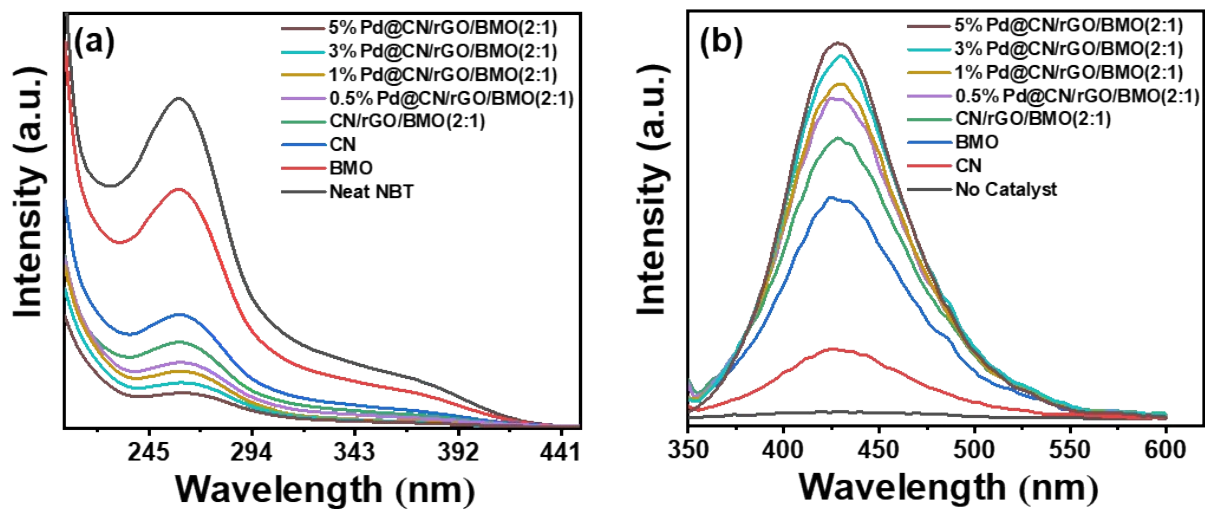


Fig. S25. (a) Comparative absorption spectra of NBT solution after light illumination for 10 min over various photocatalysts, and (b) comparative fluorescence spectra of THA solution after light illumination for 30 min over various photocatalysts.

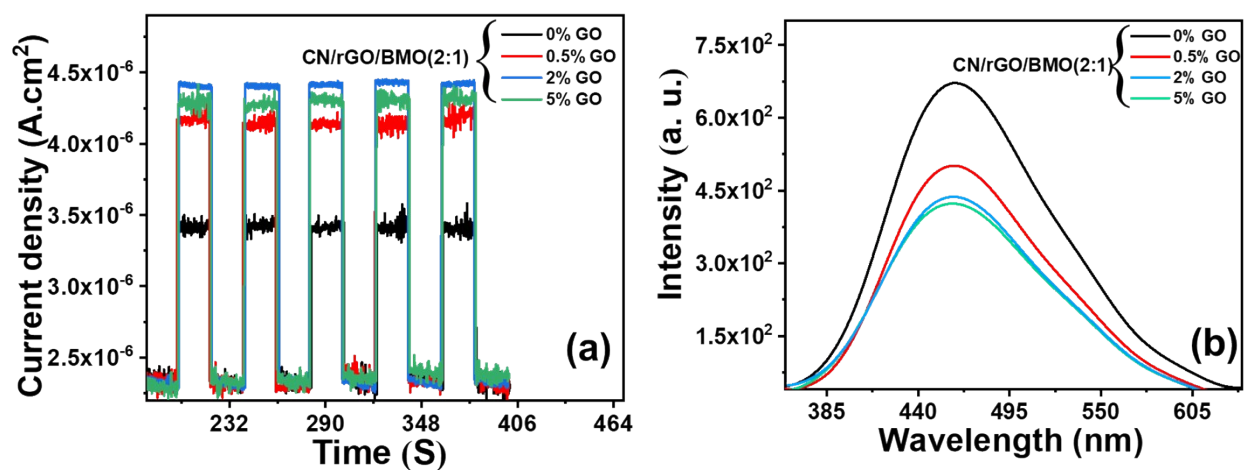


Fig. S26. (a) Transient photocurrent response, and (b) PL spectra of CN/rGO/BMO(2:1) with variation of rGO content (0%, 0.5%, 2% and 5%).

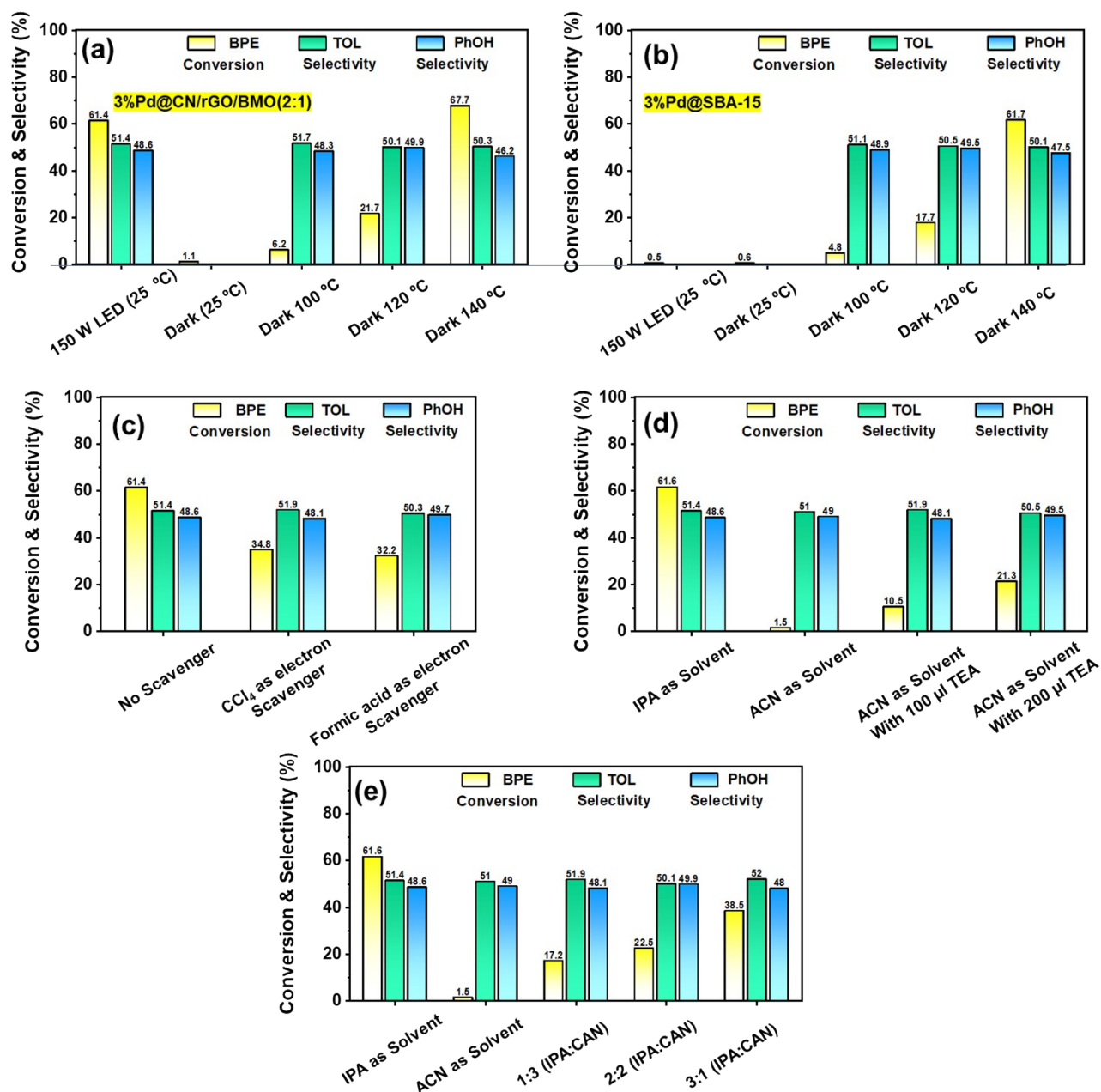


Fig. S27. Control experiments during BPE hydrogenolysis (a) reaction in light, dark, and different temperature using 3%Pd@CN/rGO/BMO(2:1), (b) reaction in light, dark, and different temperature using 3%Pd@SBA-15, (c) with using 1.5 mmol of electron scavenger, (d) in IPA, ACN and ACN + TEA, (e) in mixture of different ratio of IPA and ACN [Reaction conditions: 3%Pd@CN/rGO/BMO(2:1) (20 mg), light source (150W LED), BPE (0.1 mmol), solvent (5 ml), time (1.5 h), and H₂ (2 bar)].

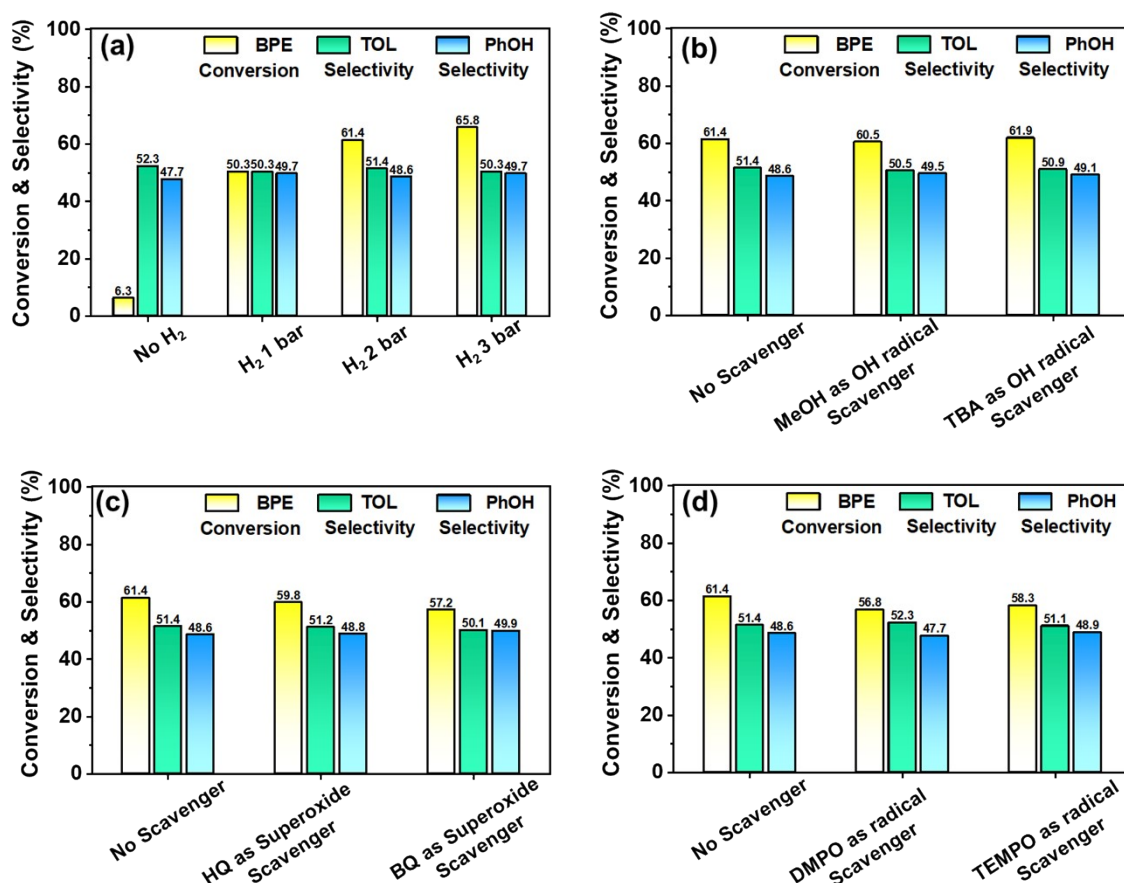


Fig. S28. Control experiments during BPE hydrogenolysis (a) reaction indifferent H₂ concentration using 3%Pd@CN/rGO/BMO(2:1), (b) with using 1.5 mmol of OH radical scavenger (c) with using 1.5 mmol of super oxide scavenger, and (d) with using 1.5 mmol of radical scavenger [Reaction conditions: 3%Pd@CN/rGO/BMO(2:1) (20 mg), light source (150W LED), BPE (0.1 mmol), solvent (5 ml), time (1.5 h), and H₂ (2 bar)].

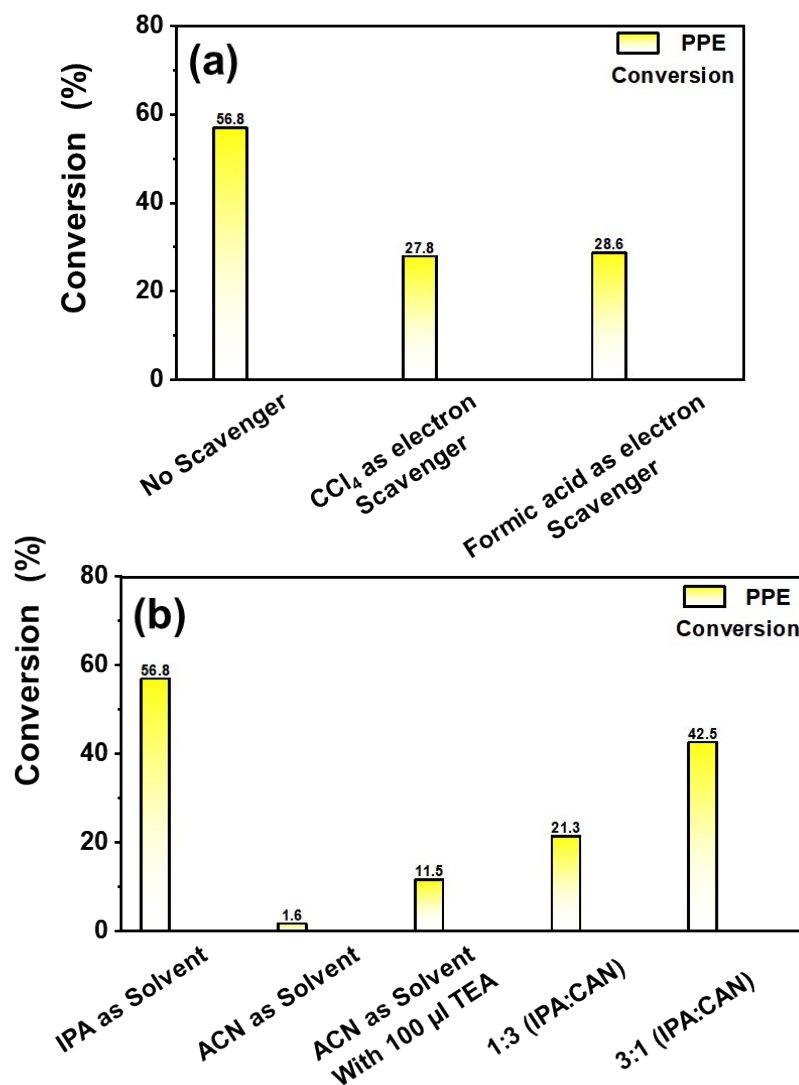


Fig. S29. Control experiments during PPE hydrogenolysis (a) with using 1.5 mmol of electron scavenger, and (b) in IPA, ACN, ACN + TEA, and mixture of different ratio of IPA and ACN [Reaction conditions: 3%Pd@CN/rGO/BMO(2:1) (20 mg), light source (150W LED), PPE (0.1 mmol), solvent (5 ml), time (8 h), and H₂ (2 bar)].

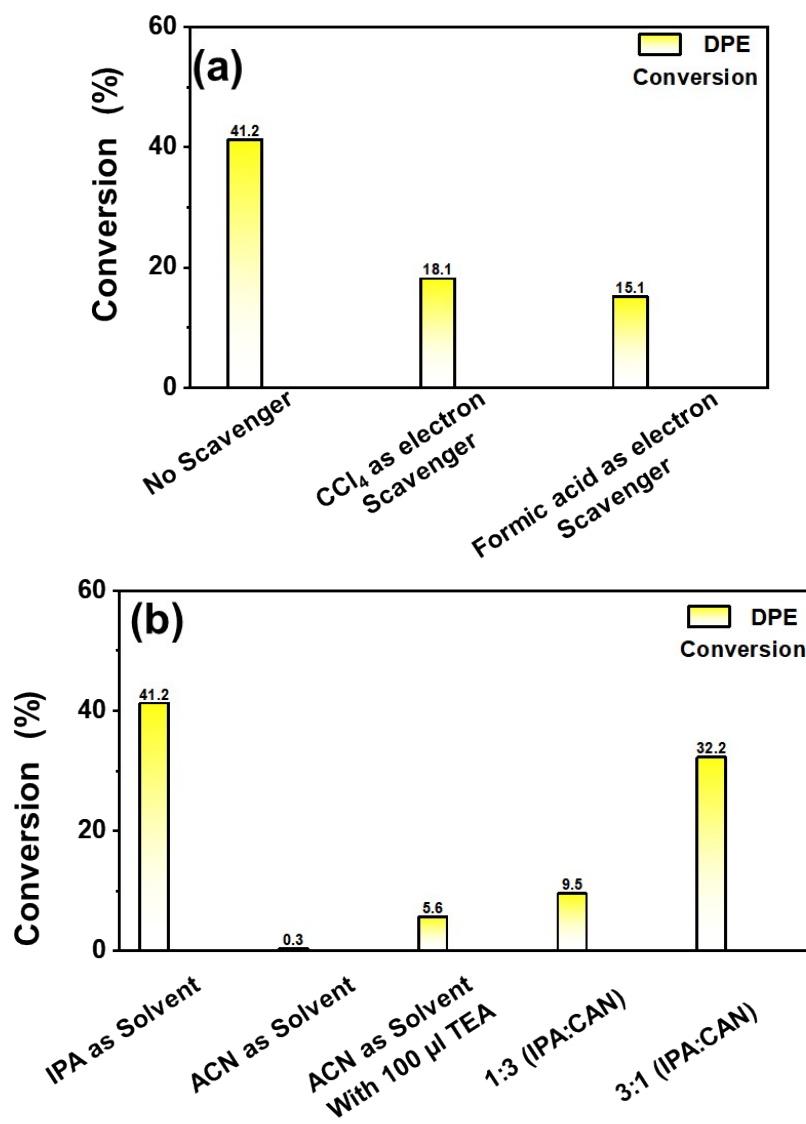


Fig. S30. Control experiments during DPE hydrogenolysis (a) with using 1.5 mmol of electron scavenger, and (b) in IPA, ACN, ACN + TEA, and mixture of different ratio of IPA and ACN [Reaction conditions: 3%Pd@CN/rGO/BMO(2:1) (20 mg), light source (150W LED), DPE (0.1 mmol), solvent (5 ml), time (16 h), and H₂ (5 bar)].

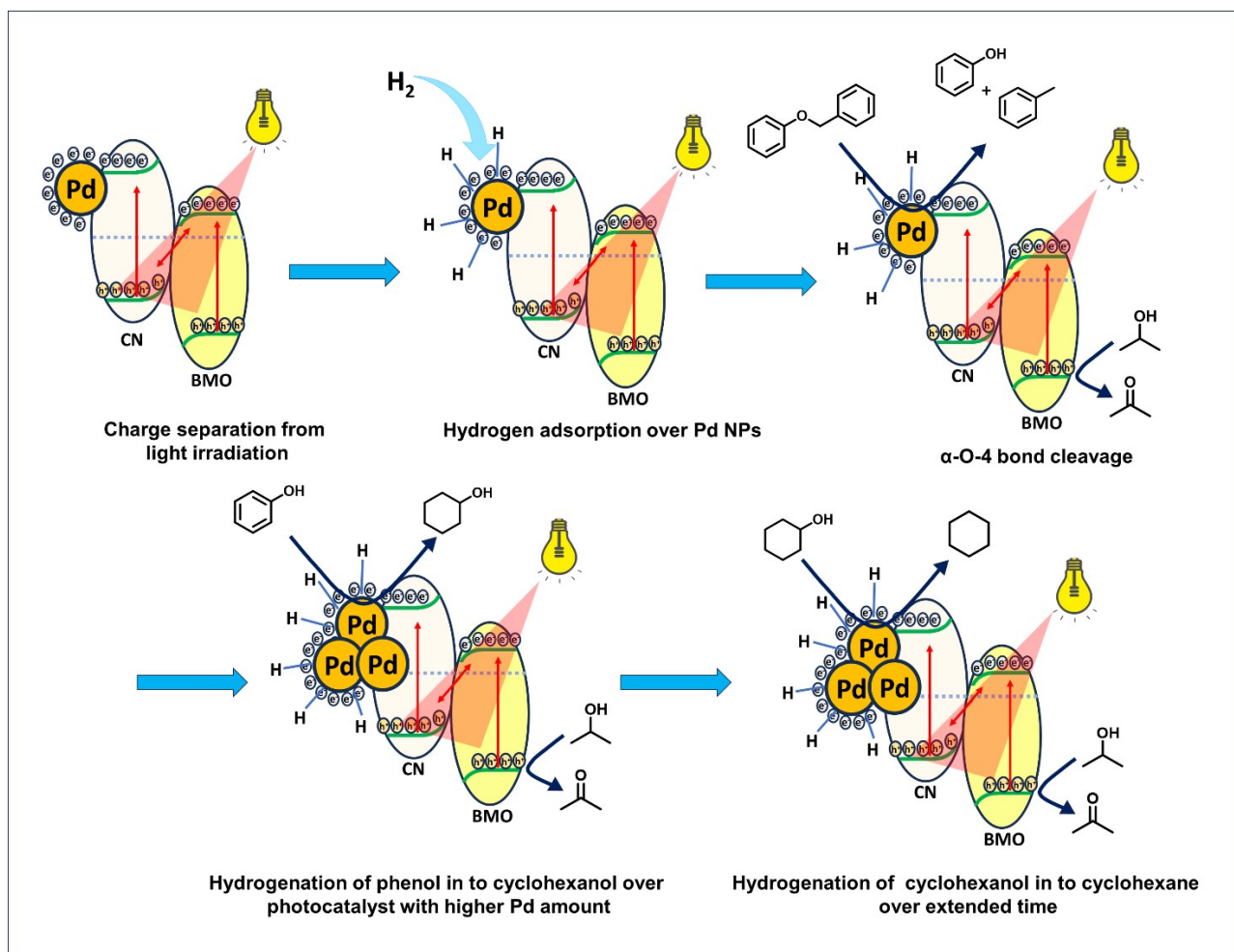


Fig. S31. A plausible mechanism for BPE photovalorisation.

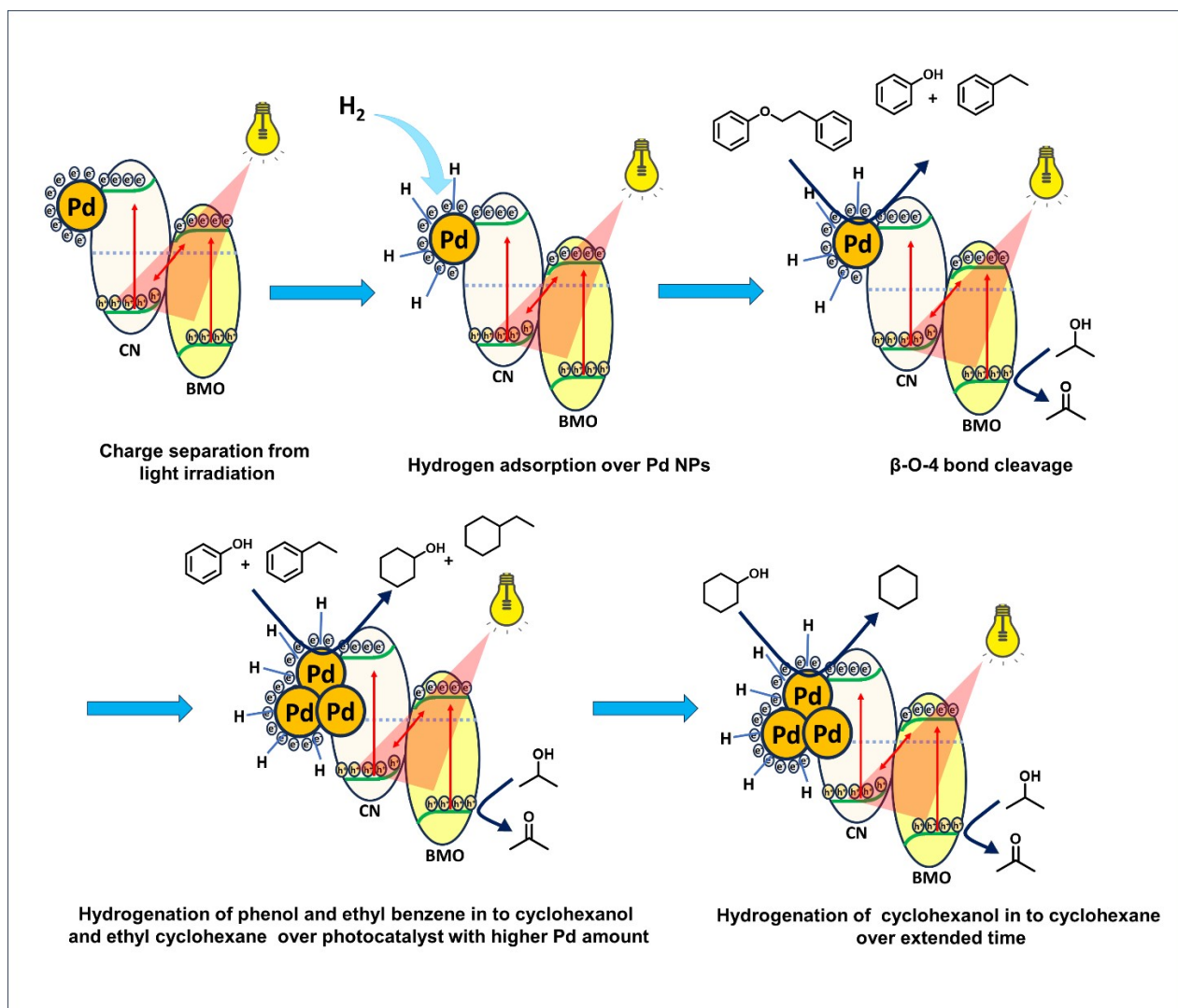


Fig. S32. A plausible mechanism for PPE photo valorisation.

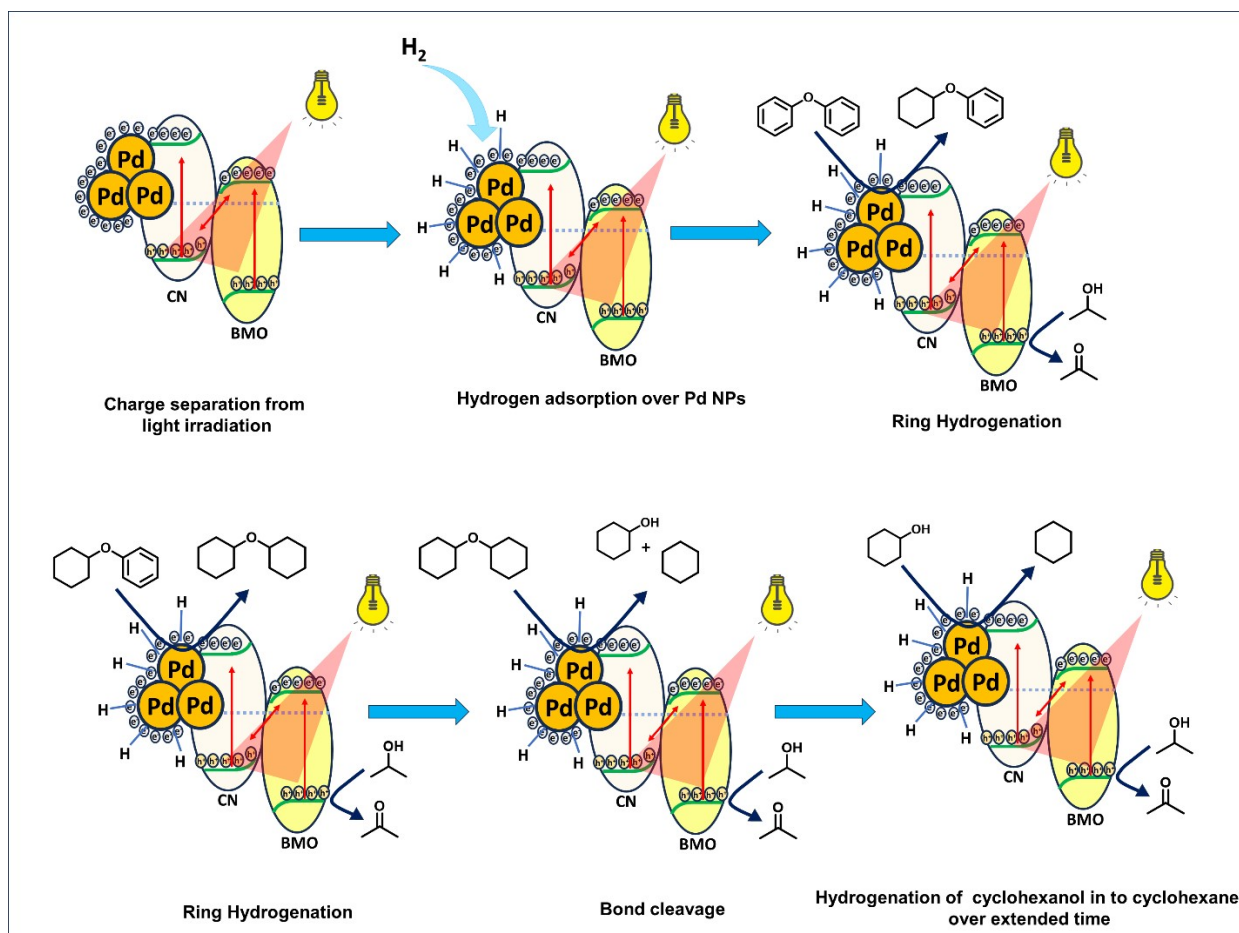


Fig. S33. A plausible mechanism for DPE photo velarization.

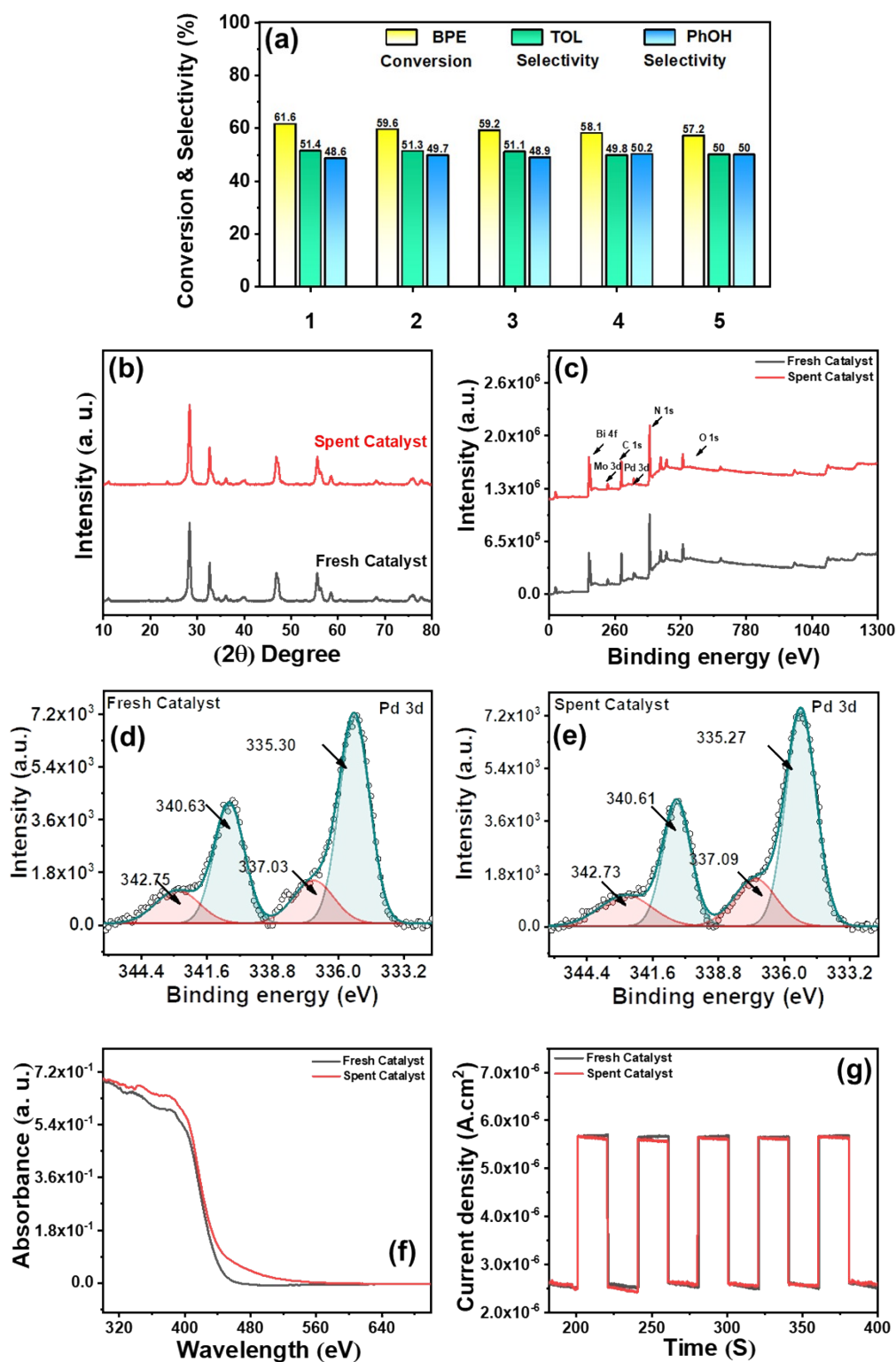


Fig. S34. (a) Catalyst recyclability conducted at half reaction starting from ~61 %conversion [Reaction conditions: BPE (1 mmol), catalyst amount (20 mg), IPA (5 mL), 150 W LED, room temperature, time 1.5 h, H₂ (2 bar)],

References

- S1 P. D. Kouris, D. J. G. P. van Osch, G. J. W. Cremers, M. D. Boot and E. J. M. Hensen, *Sustain. Energy Fuels*, 2020, **4**, 6212–6226.
- S2 P. Han, T. Tana, Q. Xiao, S. Sarina, E. R. Waclawik, D. E. Gómez and H. Zhu, *Chem*, 2019, **5**, 2879–2899.
- S3 Z. Liu, Y. Huang, G. Xiao, P. Li, H. Su, S. Sarina and H. Zhu, *Energy & Fuels*, 2021, **35**, 13315–13324.
- S4 J. Lin, X. Wu, S. Xie, L. Chen, Q. Zhang, W. Deng and Y. Wang, *ChemSusChem*, 2019, **12**, 5023–5031.
- S5 N. Luo, M. Wang, H. Li, J. Zhang, T. Hou, H. Chen, X. Zhang, J. Lu and F. Wang, *ACS Catal.*, 2017, **7**, 4571–4580.
- S6 S. Shao, K. Wang, J. B. Love, J. Yu, S. Du, Z. Yue and X. Fan, *Chem. Eng. J.*, 2022, **435**, 134980.
- S7 J. Xu, F. Lin, J. Wang and Y. Wang, *Chem. Phys. Lett.*, 2022, **805**, 139981.
- S8 G. Han, T. Yan, W. Zhang, Y. C. Zhang, D. Y. Lee, Z. Cao and Y. Sun, *ACS Catal.*, 2019, **9**, 11341–11349.
- S9 J.-Y. Wang, Z.-Z. Hu, X.-T. Sun, Y.-Q. Gao, J.-L. Wang, J. Xu and G. Jin, *Surfaces and Interfaces*, 2023, **36**, 102505.
- S10 H. Yoo, M.-W. Lee, S. Lee, J. Lee, S. Cho, H. Lee, H. G. Cha and H. S. Kim, *ACS Catal.*, 2020, **10**, 8465–8475.
- S11 J. Xu, M. Li, J. Qiu, X.-F. Zhang and J. Yao, *Int. J. Biol. Macromol.*, 2021, **185**, 297–305.
- S12 Y. Liu, Y. Guo, B. Lin, Z. Chen, X. Ying, M. Zhang, C. Wang, G. Zhang, H. Gu, D. Luo and X. Liu, *ACS Appl. Nano Mater.*, 2023, **6**, 6614–6626.
- S13 S. Tang, G. A. Baker, S. Ravula, J. E. Jones and H. Zhao, *Green Chem.*, 2012, **14**, 2922.
- S14 S. Y. Oh, D. Il Yoo, Y. Shin, H. C. Kim, H. Y. Kim, Y. S. Chung, W. H. Park and J. H. Youk, *Carbohydr. Res.*, 2005, **340**, 2376–2391.
- S15 S. K. Singh, B. M. Matsagar and P. L. Dhepe, *Biomass Convers. Biorefinery*, 2024, **14**, 5239–5249.
- S16 W. Tian, H. Li, J. Zhou and Y. Guo, *RSC Adv.*, 2017, **7**, 41176–41181.
- S17 C. G. Boeriu, D. Bravo, R. J. A. Gosselink and J. E. G. van Dam, *Ind. Crops Prod.*, 2004, **20**, 205–218.
- S18 M. J. Mehta, A. Kulshrestha, S. Sharma and A. Kumar, *Green Chem.*, 2021, **23**, 1240–1247.